Insights on the water mean transit time in a high-elevation tropical ecosystem

G. M. Mosquera[1,2], C. Segura[3], K. B. Vaché[2], D. Windhorst[4], L. Breuer[4,5] and Crespo, P.[1]

[1]{Departamento de Recursos Hídricos y Ciencias Ambientales & Facultad de Ciencias Agropecuarias, Universidad de Cuenca, Av. 12 de Abril, Cuenca, Ecuador}

[2]{Department of Biological and Ecological Engineering, Oregon State University, Corvallis, OR, USA}

[3]{Department of Forestry Engineering, Resources, and Management, Oregon State University, Corvallis, Oregon, USA}

[4]{Institute for Landscape Ecology and Resources Management (ILR), Research Centre for Biosystems, Land Use and Nutrition (IFZ), Justus Liebig University Gießen, Gießen, Germany}

[5]{Centre for International Development and Environmental Research, Justus Liebig University Gießen, Gießen, Germany}

Correspondence to: G. M. Mosquera. (giovanny.mosquerar@ucuenca.edu.ec)

Abstract

This study focuses on the investigation of the mean transit time (MTT) of water and its spatial variability in tropical high-elevation ecosystems (wet Andean páramo). The study site is the Zhurucay River Ecohydrological Observatory (7.53 km^2) located in south Ecuador. A lumped parameter model considering five transit time distribution (TTD) functions was used to estimate MTTs under steady-state conditions (i.e., baseflow MTT). We used a unique data set of the δ^{18}O isotopic composition of rainfall and streamflow water samples collected for three years (May 2011-May 2014) in a nested monitoring system of streams. Linear regression

1 between MTT and landscape (soil and vegetation cover, geology, and topography) and

2 hydrometric (runoff coefficient and specific discharge rates) variables was used to explore

3 controls on MTT variability, as well as mean electrical conductivity (MEC) as a possible

4 proxy for MTT. Results revealed that the exponential TTD function best describes the

5 hydrology of the site, indicating a relatively simple transition from rainfall water to the

6 streams through the organic horizon of the wet páramo soils. MTT of the streams is relatively

7 short (0.15-0.73 yr, 53-264 days). Regression analysis revealed a negative correlation

8 between the catchment's average slope and MTT ($R^2 = 0.78$, $p < 0.05$). MTT showed no

9 significant correlation with hydrometric variables whereas MEC increases with MTT ($R^2 =$

10 0.89 $p < 0.001$). Overall, we conclude that: 1) baseflow MTT confirms that the hydrology of

11 the ecosystem is dominated by shallow subsurface flow; 2) the interplay between the high

12 storage capacity of the wet páramo soils and the slope of the catchments provides the

13 ecosystem with high regulation capacity; and 3) MEC is an efficient predictor of MTT

14 variability in this system of catchments with relatively homogeneous geology.

15 <u>Keywords</u>: Ecohydrology, MTT, runoff generation, wet Andean páramo, tropical wetlands,

16 Histosols, Ecuador

17

18 1   Introduction

19 Investigating ecohydrological processes through the identification of fundamental catchment

20 descriptors, such as the MTT, specific discharge, evapotranspiration to precipitation ratios,

21 and others, is fundamental in order to: 1) advance global hydrological, ecological, and

22 geochemical processes understanding and 2) improve the management of water resources.

23 This is particularly critical in high-elevation tropical environments, such as the wet Andean

24 páramo (further referred as "páramo"), in which, hydrological knowledge remains limited,

25 despite its importance as the major water provider for millions of people in the region (De

26 Bièvre and Calle, 2011; IUCN, 2002). Water originated from the páramo sustains the socio-

27 economic development in this region by fulfilling urban, agricultural, industrial, and

28 hydropower generation water needs (Célleri and Feyen, 2009). Here we focus on the MTT of

29 water, which we define as the average time elapsed since a water molecule enters a catchment

1   as recharge to when it exits it at some discharge point (Bethke and Johnson, 2002; Etcheverry

2   and Perrochet, 2000; Rodhe et al., 1996).

3   Despite the importance of tropical biomes as natural sources and regulators of streamflow,

4   there are very few studies of MTT in tropical environments (e.g., Farrick and Branfireun,

5   2015; Muñoz-Villers et al., 2015; Roa-García and Weiler, 2010; Timbe et al., 2014). The

6   majority of MTT studies have been conducted in catchments with strong climate seasonality,

7   i.e., located in the northern and southern hemispheres (e.g., Lyon et al., 2010; McGlynn and

8   McDonnell, 2003; McGuire et al., 2005), and considerably less attention has been devoted to

9   tropical environments. Most tracer-based studies conducted in tropical latitudes focused on

10   isotope hydrograph separation at storm event scale (e.g., Goller et al., 2005; Muñoz-Villers

11   and McDonnell, 2012), the isotopic characterization of precipitation patterns (e.g., Vimeux et

12   al., 2011; Windhorst et al., 2013), and the identification of ecohydrological processes (e.g.,

13   (Crespo et al., 2012; Goldsmith et al., 2012; Mosquera et al., 2016). However, studies

14   focusing on MTTs in order to improve the understanding of rainfall-runoff processes and their

15   dependence on landscape biophysical features in tropical regions are still lacking and urgently

16   needed in order to improve water resources management.

17   The páramo is widely recognized by its high runoff regulation capacity (i.e., páramo water

18   yield is sustained year-round regardless of precipitation inputs) (Buytaert et al., 2006; Célleri

19   and Feyen, 2009). However, efforts to investigate the processes that control such hydrological

20   behavior are scarce. Recent investigations in our study site suggest that runoff originates from

21   the shallow organic horizon of the páramo soils located near the streams (Histosol soils or

22   Andean wetlands), thus favoring shallow subsurface flow. On the contrary, deep groundwater

23   contributions to discharge are minimal and saturation excess overland flow (even in the nearly

24   saturated Histosol soils) rarely occur (Buytaert and Beven, 2011; Crespo et al., 2011). The

25   hydrological importance of shallow subsurface flow to runoff generation has also been

26   demonstrated in a variety of ecosystems around the globe (e.g., Freeze, 1972; Hewlett, 1961;

27   Penna et al., 2011), but yet, MTTs have not been explored in these systems. Our study site

28   provides a unique opportunity to gain understanding of the MTT of a shallow subsurface flow

29   dominated system in a tropical setting. In addition, the study of the MTT in natural wetland

1 systems has been limited to sites located in northern boreal catchments in Sweden (Lyon et

2 al., 2010), and peatlands in Scottish mountainous regions (e.g., Hrachowitz et al., 2009a;

3 Tetzlaff et al., 2014). While streams draining these catchments have significant contributions

4 from spring snowmelt and groundwater, respectively, neither of these allows for the isolation

5 of the effect of wetlands in the shallow subsurface and/or near surface (i.e., overland flow)

6 transport of the water within the catchments.

7 Another critical issue is the identification of controls on MTT variability. As detailed

8 observations of combined hydrometric and isotopic information are not feasible in many

9 regions due to limited funding and site accessibility, identifying controls of MTT variability

10 in nested and paired monitoring systems of streams is fundamental towards regionalization of

11 ecohydrological processes (Hrachowitz et al., 2009a) and prediction in ungauged basins

12 (Tetzlaff et al., 2010). Yet, investigation of controls on MTT variability is still fairly scarce

13 (Tetzlaff et al., 2013). Most studies have found that MTT scales with topographic and/or

14 hydropedological controls. For instance, topographical controls on MTT variability were

15 found in New Mexico, USA catchments (slope direction and exposure) (Broxton et al., 2009)

16 and a system of streams in Oregon, USA (ratio between flow path length and flow path

17 gradient) (McGuire et al., 2005); whereas the proportion of wetlands and responsive soils

18 were reported as major MTT controls in Swedish catchments (Lyon et al., 2010) and Scottish

19 streams (Soulsby et al., 2006), respectively.

20 In the last few decades, MTT modeling has been conducted applying an approach that

21 assumes steady-state conditions in the hydrologic systems, i.e., the lumped convolution

22 approach (LCA) (Amin and Campana, 1996; Maloszewski and Zuber, 1996). However, this

23 assumption is often violated as a result of strong climate seasonality and heterogeneities in the

24 landscape configuration and hydropedological distribution of catchments (Kirchner, 2016a,

25 2016b). This has led to a growing recognition of the time-variant nature of transit times (e.g.,

26 Birkel et al., 2015; Harman, 2015; Hrachowitz et al., 2013), which a number of studies have

27 begun to explore. Most of this initial work has yielded results with high degree of uncertainty

28 (Harman, 2015; Klaus et al., 2015; McMillan et al., 2012), or uncertainty has not been

29 estimated (Davies et al., 2013; Heidbüchel et al., 2012; van der Velde et al., 2015) as a result

4

of expensive computation costs or high uncertainties related to the spatial variability of the input hydrometric and tracer field measurements. It is clear however, that given the mathematical limitations (Duvert et al., 2016; Seeger and Weiler, 2014), the high-temporal resolution of tracer data (Harman, 2015; Heidbüchel et al., 2012), and the general unavailability of long-term tracer records (Hrachowitz et al., 2010; Klaus et al., 2015) required for hydrological modeling under non-stationary conditions, the LCA remains to be a useful methodology for MTT estimation. This holds true not only in understudied regions such as the tropics (e.g., Farrick and Branfireun, 2015; Muñoz-Villers et al., 2015; Timbe et al., 2014), but also elsewhere (e.g., Duvert et al., 2016; Hale and McDonnell, 2016; Hale et al., 2016; Hu et al., 2015; Seeger and Weiler, 2014).

Given the relatively homogenous landscape features and very low seasonality in the hydrometeorological conditions in our páramo site, applying the LCA to our unique water stable isotopic dataset represents a robust first step to build-up improved catchment functioning understanding using hydrometric-tracer based hydrologic modeling. To our knowledge, this is the first contribution regarding the modeling of MTT in páramo ecosystems specifically, and more generally in regions with low climate seasonality and catchments with low degree of heterogeneity. Future efforts building on the monitoring infrastructure and continuously collected datasets will allow for continual improvement in hydrologic interpretation, eventually incorporating alternative modeling techniques that explicitly recognize non-stationarity and storage dynamics in the hydrological behavior of this tropical ecosystem (e.g., Birkel et al., 2015; Harman, 2015; Hrachowitz et al., 2013).

In this study, we seek to add to the current geographical scope of MTT studies by addressing two questions which remain open in hydrological science, and have received little attention in high-elevation tropical ecosystems: "How old is stream water?" (McDonnell et al., 2010) and "How does landscape structure influence catchment transit time across different geomorphic provinces?" (Tetzlaff et al., 2009). Detailed hydrometric observations highlighting subsurface dominated rainfall-runoff response (Crespo et al., 2011; Mosquera et al., 2016) together with information of the landscape biophysical characteristics in our páramo study site will allow for process-based understanding regarding: i) the spatial variability of baseflow MTTs and ii)

the factors controlling such variability. Based on our current knowledge of the hydrology of the ecosystem, in particular, the apparent dominance of shallow subsurface flow to runoff generation, we hypothesize relatively short baseflow MTTs compared to systems dominated by groundwater contributions to discharge. Also, based on the hydropedological and climatic similarities between our páramo site and the peatland-podzols dominated ecosystems in the Scottish highlands (e.g., Soulsby et al., 2006; Tetzlaff et al., 2014), we hypothesize the proportion of wetlands to be a dominant control on the variability of the MTT in this high-elevation tropical ecosystem.

2 Materials and methods

2.1 Study site

The Zhurucay River Ecohydrological Observatory is a basin located within a tropical alpine biome, locally known as wet Andean páramo. It is situated in south Ecuador (3º04'S, 79º14'W) on the west slope of the Atlantic-Pacific continental divide and discharges into the Jubones River (Pacific Ocean tributary). The basin has a drainage area of 7.53 km^2 and extends within an elevation range of 3400 to 3900 m a.s.l. Climate is mainly influenced by the Pacific Ocean regime and to a lesser degree to the continental air masses from the Amazon basin. Mean annual precipitation at the observatory is 1345 mm at 3780 m a.s.l. Precipitation shows low seasonality with two relatively drier months (August and September) and primarily falls as drizzle (Padrón et al., 2015). Mean annual temperature is 6.0 °C at 3780 m a.s.l. and 9.2 °C at 3320 m a.s.l. (Córdova et al., 2015).

The geology of the region is characterized by volcanic rock deposits compacted by glacial activity during the last ice age (Coltorti and Ollier, 2000). The Quimsacocha formation, composed by basaltic flows with plagioclases, feldspars, and andesitic pyroclastics, covers the northern part of the basin. The Turi formation covers the southern part of the catchment and its lithology mainly corresponds to tuffaceous andesitic breccias, conglomerates, and horizontally stratified sands. Both formations date from the late Miocene period (Pratt et al., 1997). The geomorphology of the landscape bears the imprint of glaciated U-shaped valleys. The average slope of the basin is 17%. The majority of the basin (72%) has mean gradients

between 0-20 %, although slopes up to 40% are also found (24%). There is an interesting geomorphic feature in the northeastern side of the basin corresponding to a ponded wetland at a flat hilltop. As indicated by geologists from INV metals mining company, this structure most likely resulted from the eutrophication of a lagoon due to high accumulation of volcanic material. This area is locally known as "Laguna Ciega" ("Blind Lagoon" in Spanish) and drains towards the outlet of catchment M7 (see Figure 1). The analysis of the water stable isotopic composition of soil water and streamflow in this area indicated that the hydrologic processes of this site occur in the shallow ponded water that is directly connected to the drainage network; while deeper water stored in the soil profile has little influence for discharge generation most likely as a results of the eutrophic condition of the wetland (Mosquera et al., 2016).

Andosols are the dominant soil type in the study site. They cover approximately 80% of the total basin area and are mainly found in the hillslopes. Histosols (Andean wetlands) cover the remaining portion of the basin and are mainly found in flat areas where rock geomorphology allows water accumulation (Mosquera et al., 2015). These soils, formed from the accumulation of volcanic ash in flat valley bottoms and low gradient slopes, are black, humic, and acid soils rich in organic matter with low bulk density and high water storage capacity (Quichimbo et al., 2012). The organic fraction of the Histosol soils corresponds to an H horizon (median depth 76.5 cm); while in the Andosol soils it corresponds to an Ah horizon (median depth 40cm). The mineral fraction of both soils corresponds to a C horizon (median depth of 31 cm in the Histosols and 40 cm in the Andosols). A complete description of soil properties can be found in Mosquera et al. (2015) and Quichimbo et al. (2012). Vegetation coverage is highly correlated with the soil type. Cushion plants (such as *Plantago rigida, Xenophyllum humile, Azorella spp.*) grow primarily in Histosols, while tussock grass (mainly *Calamagrostis* sp.) (Ramsay and Oxley, 1997; Sklenar and Jorgensen, 1999) grow in Andosols. The main landscape characteristics are summarized in Table 1.

2.2 Hydrometric information

Discharge and precipitation were continuously monitored since October 2010. A nested monitoring network was used to measure discharge. The network consisted of seven tributary catchments (M1 to M7) draining to the outlet of the basin (M8). Catchments M1 to M6 comprise the main stream network draining towards the outlet of the Zhurucay basin (M8), whereas catchment M7 is a small catchment originating in a ponded wetland at a flat hilltop (Figure 1). V-notch weirs were constructed to measure discharge at the outlet of the tributaries M1-M7 and a rectangular weir at the outlet of the basin M8. Each catchment was instrumented with pressure transducers (Schlumberger DI500) with a precision of ±5 mm. Water levels were recorded at a 5-minute resolution, and transformed into discharge using the Kindsvater-Shen relationship (U.S. Bureau of Reclamation, 2001). The discharge equations were calibrated by applying the constant rate salt dissolution technique (Moore, 2004). Precipitation was recorded using tipping buckets with a resolution of 0.2 mm at two stations located at 3780 and 3700 m a.s.l. (Figure 1).

2.3 Collection and analysis of water stable isotopic and electrical conductivity data

We used a three-year record (May 2011 – May 2014) of ^{18}O and ^{2}H isotopic compositions of water samples collected in precipitation and streamflow. Data were collected at different resolutions, from event-based to biweekly, given logistic constraints and opportunities. Higher resolution data were aggregated to biweekly using precipitation weighted means for record consistency. The same nested monitoring network used for measuring discharge was implemented for stable isotopes in streamflow at the seven tributary catchments M1 to M7, and including M8 at the outlet of the basin. Water samples in precipitation were collected using two rain collectors located at 3780 and 3700 m a.s.l. Each collector consisted of a circular funnel and a polypropylene bottled covered with aluminum foil. Evaporation was prevented by placing a plastic sphere (4 cm diameter) in the funnel and a layer of 0.5 cm mineral oil within the polypropylene bottle. Due to the sampling procedure and the local climate, kinetic fractionation by evaporation can be neglected and hence both stable isotopes

1   yield the same results (Mosquera et al., 2016). Therefore only the results using the isotopic

2   composition of ^{18}O are reported. Rainwater samples are cumulative representations of the

3   isotopic signature between sampling dates while stream grab water samples represent discrete

4   points in time. The collected water samples were stored in 2 ml amber glass bottles, covered

5   with parafilm, and kept away from the sunlight to prevent fractionation by evaporation as

6   recommended by the International Atomic Energy Agency (Mook, 2000). The isotopic

7   composition of the water samples was measured using a cavity ring-down spectrometer

8   L1102-i (Picarro, USA) with a 0.5‰ precision for deuterium (^{2}H) and 0.1‰ precision for

9   oxygen-18 (^{18}O). Isotopic concentrations are presented in the δ notation and expressed in per

10   mill (‰) according to the Vienna Standard Mean Ocean Water (V-SMOW) (Craig, 1961).

11   Electrical conductivity (EC) was measured directly in-stream simultaneously with the water

12   isotopic data starting in 2012, the second year of the monitoring period. EC was measured

13   using the digital conductivity sensor Tetracon 925 (WTW, Germany) with a precision of ±

14   0.5%.

15   **2.4   Mean transit time modeling and transit time distributions**

16   As a result of the homogeneous landscape and hydrometeorological conditions in the

17   Zhurucay basin, we estimated mean transit times (MTTs) using an inverse solution of the

18   LCA (Amin and Campana, 1996; Małoszewski and Zuber, 1982), which assumes steady-state

19   conditions. The LCA seeks for the parameter set of the model that best describes the

20   hydrologic system represented by a predefined transit time distribution (TTD) function

21   (Maloszewski and Zuber, 1996). The TTD describes the transition of an input signal (e.g.,

22   precipitation, snow) of tracer (e.g., δ^{18}O, δ^2H) to the signal at an outlet point (e.g.,

23   groundwater, streamflow) resulting from the subsurface transport of water molecules within a

24   catchment. Mathematically the TTD is described by a convolution integral that transforms the

25   input signal (δ_{in}) into an output signal (δ_{out}), considering a time lag between them ($t - \tau$)

26   through a transfer function (TTDs or $g(\tau)$) describing the subsurface transport of tracer as

27   follows:

$$\delta_{out}(t) = \int_0^\infty g(\tau)\,\delta_{in}(t-\tau)\,d\tau \quad (1)$$

where τ is the integration variable representing the MTT of the tracer. A more robust
approximation weights the isotopic concentration of the input by considering recharge mass
variation ($w(\tau)$) so that the outflow composition reflects the mass flux leaving the catchment:

$$\delta_{out}(t) = \frac{\int_0^\infty g(\tau)\,w(t-\tau)\,\delta_{in}(t-\tau)\,d\tau}{\int_0^\infty g(\tau)\,w(t-\tau)\,d\tau} \quad (2)$$

where $w(t-\tau)$ can be described in terms of rainfall magnitude, intensity, or effective
precipitation (McGuire and McDonnell, 2006). Precipitation intensity was used to volume
weight the isotopic composition of precipitation in our study. Recharge was represented by
the rainfall isotopic composition weighted by precipitation rate and accounted for relatively
small recharge (i.e., lower precipitation inputs) during the less wet months (August and
September).

MTT was estimated by adjusting the response function or TTD to fit the measured and
simulated stream water isotopic composition. Five TTDs were considered to describe the
subsurface transport of water molecules in the Zhurucay basin. We used the exponential
model (EM), exponential-piston flow model (EPM), the dispersion model (DM)
(Małoszewski and Zuber, 1982), the gamma model (GM) (Kirchner et al., 2000), and the two
parallel linear reservoir model (TPLR) (Weiler et al., 2003). Each model is briefly described
below and Table 2 summarizes their equations, fitting parameters, and the range of initial
parameters used in this study.

The EM represents a well-mixed system and assumes contributions from all flow paths. It
assumes a relatively simple transition of the tracer towards the stream network. The EPM is
an extension of the EM in which a delay in the shortest flow paths is assumed by the piston
flow portion of the system. In addition to the MTT, it has an additional fitting parameter (η),
which represents the ratio of the total volume to the volume represented by the exponential
distribution. The DM arises from the solution of the one-dimensional advection-dispersion
equation (Kreft and Zuber, 1978) and assumes that there is influence of hydrodynamic

10

1   dispersion in the system's flow paths. It also has two fitting parameters, the MTT and the

2   dispersion parameter (Dp), which relates to the tracer transport process. The GM is a more

3   flexible and general version of the exponential model in which the product of two parameters

4   provides an estimation of the MTT of the system. These parameters are the shape parameter

5   (α) and the scale parameter (β) (Kirchner et al., 2000). The TPLR represents two parallel

6   reservoirs each one represented by a single exponential distribution. It has three fitting

7   parameters, the MTT of the slow (MTT_s) and fast (MTT_f) reservoirs and a parameter

8   representing the fraction of each of them with respect to total flow (φ) (Weiler et al., 2003).

9   The MTT approach is based on the following assumptions: 1) the tracer concentration is

10   conservative (i.e., the tracer does not react with other elements present in the system); 2) the

11   input tracer concentration is input in flux mode (i.e., volumetrically weighted); 3) the tracer

12   enters the system only once and uniformly; 4) a representative tracer input can be identified;

13   5) transport of solute is one-dimensional and represented by a single TTD; and 6) there is a

14   uniform storage of water within the catchment (i.e., steady-state of the flow in the system)

15   (Małoszewski and Zuber, 1982). The steady-state assumption is valid for humid environments

16   during specific flow characteristics (i.e., baseflow) (McGuire et al., 2002). In order to comply

17   with the latter assumption, streamflow water samples collected during extreme rainfall events

18   were excluded for the MTT simulations (McGuire and McDonnell, 2006; Muñoz-Villers et

19   al., 2015). As a result, estimates correspond to baseflow MTTs, hereafter simply referred to as

20   MTT. To obtain more stable results, we looped the available three years of isotopic data ten

21   times during calibration in order to extend the data series for 30 years as a warm-up period

22   following Hrachowitz et al. (2011) and Timbe et al. (2014).

23   **2.5   Model performance and uncertainty analysis**

24   The model performance was evaluated using the Kling–Gupta efficiency coefficient (KGE)

25   (Gupta et al., 2009). KGE ranges from -∞ to 1, where unity indicates an ideal optimization.

26   KGE can be viewed from a multi-objective perspective because it accounts for correlation

27   (i.e., balancing dynamics, r), variability error (γ), and bias error (β) within a single objective

28   function. The efficiency is mathematically represented by the Euclidean distance (ED) in each

29   of the three dimensions (r, γ, and β) to an ideal point where all of them are maximized (i.e.,

where ideally the three factors are set to one). Efficiencies lower than 0.45 were considered poor predictions (Timbe et al., 2014).

Depending on the TTD function used, 1 to 3 parameters were fitted during the simulations. Models were built using parameter sets generated through a uniform Monte Carlo sampling procedure (Beven and Freer, 2001). Each model was first run 10,000 times within a wide range of parameter values (Table 2). Once a parameter value that yielded the best KGE was clearly identified, the model was run again within a narrowed range of parameters until obtaining at least 1,000 behavioral solutions (i.e., solutions corresponding to at least 95% of the highest KGE) (Timbe et al., 2014) and their 5 and 95% limit bounds (i.e., 90% confidence interval) were estimated using the Generalized Likelihood Uncertainty Estimation methodology (GLUE) (Beven and Binley, 1992). The Akaike Information Criterion (AIC, Akaike, 1974) was used as a parsimoniousness metric for model selection that penalizes model performance based on the number of fitted parameters used to calibrate each model. The model with the lowest AIC is the most efficient at fitting the observed values. The measure of identification (MI) (Segura et al., 2012) was calculated as a metric of the model parameter identifiability. The MI is defined as the ratio between the behavioral parameters range to the initial range (based on Timbe et al., 2014) and indicates how well a parameter is identified. This metric is expressed as a percentage and by definition, the smaller the value, the better the parameter identifiability. We considered a parameter is well-identified if its MI is lower than 10%. The best model describing the hydrologic conditions of the system was selected using the following criteria: 1) best goodness of fit using the KGE criterion, 2) lowest AIC, 3) results that yielded the lower uncertainty estimations, and 4) higher parameter identifiability using the MI criterion.

2.6   Correlation analysis of MTT and catchment characteristics

We used linear regression to investigate relations between landscape characteristics and hydrological behavior with the MTT of the catchments. For this analysis, we included the catchments which comprise the main drainage network (i.e., catchments M1 to M6) and the catchment outlet (M8) given that they possess comparable hydropedological and geomorphological characteristics. That is, catchments situated at the valley bottom have well-

12

1 defined interconnections between wetlands in the riparian areas and the surrounding Andosol

2 soils at the slopes. Catchment M7 on the other hand, is located at a flat hilltop at the outlet of

3 a wetland area which remains ponded throughout the year. The geomorphology of this

4 concave (lagoon shaped) structure and its ponded eutrophic condition has allowed for the

5 hydrologic processes to mainly occur in the shallowest ponded portion of the water directly

6 connected to the stream network (with little influence of the most likely immobile water

7 which remains stored in the deeper soil fraction) (Mosquera et al., 2016). Therefore, its

8 hydrological response is not comparable to the other catchments where hydrologic processes

9 mainly occur in the soils and consequently was excluded from the regression analysis.

10 Statistical significance of the correlations was tested using the F-test at a 95% confidence

11 level (i.e., $p < 0.05$).

12 The landscape and hydrometric variables tested for correlation were obtained from previous

13 studies at the site (Mosquera et al., 2015) and from detailed soil, vegetation, and topographic

14 information provided by INV Metals. The landscape features considered were: soil type,

15 vegetation, geology, catchment size, slope, flow path length and gradient, and topographic

16 wetness index (TWI) (Beven and Kirkby, 1979b) (Table 1). The hydrometric variables

17 considered were: annual runoff, annual precipitation, runoff coefficient, and streamflow rates

18 (Table 3). Weekly collected EC for three years (June 2012-June 2015) was averaged and also

19 tested for correlation with MTT.

3   Results

3.1   Hydrologic and isotopic characterization in rainfall and streamflow

22 Precipitation in the Zhurucay basin is evenly distributed throughout the year (Figure 2a),

23 except for two months with relatively lower precipitation inputs (i.e., August and September),

24 both accounting for less than 8% of total annual precipitation. Spatially, annual precipitation

25 (P) is evenly distributed across the basin with an average of $1,275 \pm 9$ mm. Total annual

26 runoff (Q) is spatially more heterogeneous, varying between 684 and 864 mm per year.

27 Runoff coefficients (Q/P) show relatively low spatial variability between 0.55 and 0.68 (Table

28 3). The hydrograph at the outlet of the basin (M8) also depicts a flashy response to

1 precipitation inputs, even during these less humid months (see zoom in Figure 2a). Similar

2 behavior is observed at all catchments.

3 The δ^{18}O isotopic composition in rainfall is highly variable throughout the year (e.g., average

4 -10.2 ± 0.32‰ at the upper station) (Figure 2b) and follows a seasonal pattern with

5 isotopically enriched values during highest precipitation rates (April-May), and isotopically

6 depleted values in the less humid period (August-September). The δ^{18}O isotopic composition

7 in streamflow collected during low flows on the other hand, is much more damped (average -

8 10.0 ± 0.06‰, at M8) than the isotopic composition in precipitation (Table 4).

9 ## 3.2   TTD evaluation and selection

10 In order to identify the TTD that best describes the hydrologic system in the Zhurucay basin,

11 we tested and evaluated the performance of all TTDs at all catchments. Considering that

12 similar results were obtained for all catchments and for brevity, only results for M8, the basin

13 outlet, are shown.

14 All TTDs reproduce the δ^{18}O isotopic composition at the outlet of the basin (M8) with

15 efficiencies varying between 0.50 and 0.76, i.e., above the threshold of model acceptance

16 (KGE > 0.45) (Table 5). The more flexible models, GM and TPLR yield the highest

17 performances with KGEs of 0.75 and 0.76, respectively. The EM and the EPM yield similar

18 efficiencies (KGE = 0.63), while the DM yields the lowest efficiency among all (KGE =

19 0.50). The models associated with the highest KGEs yield the highest uncertainty bounds

20 according to their threshold of behavioral solutions; whereas the EM shows the lowest

21 uncertainty (Figure 3). The model parsimoniousness analysis evaluated using the AIC

22 indicates that the EM (AIC = 2.92) is the best model structure, whereas higher AIC values

23 were determined for all model with more than one fitting parameters (GM, 4.58; EPM, 4.92;

24 DM, 5.39; TPLR, 6.55). The models' parameter identification analysis indicates that even

25 though the TPLR model yields the highest KGE, the level of identification of its parameters is

26 the poorest (Figure 4). The identification metric (IM, i.e., the ratio of the behavioral to the

27 initial parameter ranges, Table 5) yields high values for all parameters for the TPLR model

28 (MIs ranges between 31% and 85%). For the EPM and GM models one parameter is well

29 identified (MIs < 10%), while the others show higher MI values. For the DM, both parameters

14

1 are not well identified. The MI for the single parameter that defines the EM is very strong (MI

2 = 4%). This coupled analysis of model efficiency and parsimoniousness in combination with

3 parameter identifiability indicates that although models with a higher number of fitting

4 parameters provide higher efficiencies, their parameters are more uncertain.

5 Taking into account the goodness of fit, parsimoniousness, uncertainty bounds, and the

6 identifiability of the models' parameters, the EM is the model that best describes the temporal

7 variability of the baseflow $\delta^{18}O$ isotopic composition across the Zhurucay basin. It is also

8 clear that the higher efficiencies yielded by the more flexible models, GM and TPLR, result

9 from a higher number of fitting parameters rather than from a more realistic representation of

10 the hydrologic functioning of the catchments. The EM was also found to describe the

11 subsurface transport of water in another system of catchments in eastern Mexico, where soil

12 have predominantly formed by volcanic ash accumulation (Muñoz-Villers et al., 2015).

13 The EM represents a well-mixed reservoir with relatively simple transition of the water (i.e.,

14 tracer) in the subsurface towards the stream network. In the Zhurucay basin, the organic and

15 porous páramo soils allow for the efficient mixing of water within the whole profile of these

16 poorly developed soils. This effect particularly occurs in the Histosols (Andean wetlands)

17 which are directly connected, hydrologically, to the drainage network (Mosquera et al., 2016).

18 These factors result in a relatively simple transition of infiltrated precipitation from a well-

19 mixed reservoir towards the catchment outlet. This process-based analysis of physical

20 characteristics of the system further support the EM as the model that best describes the

21 transport of water across the Zhurucay basin.

22 **3.3 Baseflow MTT**

23 Results of the EM for selected catchments with the longest (M3), intermediate (M6), and

24 lowest (M7) MTTs are shown in Figure 5 and statistics of the EM simulations at all

25 catchments are summarized in Table 6. The EM overcomes the modeling acceptance criterion

26 of KGE > 0.45 at all catchments with KGE values ranging between 0.48 and 0.84. The

27 longest MTTs is found in catchment M3 (0.73 years, 264 days) whereas the shortest at M7

28 (0.15 years, 53 days). The MTT for the other catchments vary within this range. On average,

29 within the 90% confidence level for the catchments forming the main drainage network (M1-

1   M6 and M8), MTT estimations show small variations (25 days at the lower confidence bound

2   and 35 days at the upper confidence bound) with small standard deviation (4 days for the

3   upper bound and 6 days for the lower bound). For catchment M7, variations are even smaller

4   (9 days at the lower confidence bound and 11 days at the upper confidence bound). In

5   addition, the model performs best for catchments with high variability in their isotopic

6   composition during the monitoring period. For instance, catchment M3 (Figure 5a) shows the

7   smallest amplitude in isotopic variation for the observed and simulated data (Table 6),

8   coupled with the lowest KGE (0.48) and the highest MTT. On the other hand, catchment M7

9   (Figure 5c) shows the highest amplitude in isotopic variation for the observed and simulated

10   data, coupled with the highest KGE (0.84) and the shortest MTT. Similarly, catchment M6

11   (Figure 5b), which has a MTT shorter than the one in M3 and longer than the one in M7, has

12   an amplitude and KGE varying between the ones in M3 and M7. The Monte Carlo

13   simulations for the fitted parameter MTT (Figure 5) clearly depict how the MTT which yield

14   the highest KGE in each catchment decreases as the variation in their isotopic composition

15   increases as described above. Results from all the catchments are also described by this trend.

16   The MTT probability density functions (PDFs), which indicate the distribution of MTTs in

17   the hydrologic system, and cumulative density functions (CDFs), which express the tracer

18   ''mass recovery from an instantaneous, uniform tracer mass addition" (McGuire et al., 2005)

19   based on the fitted parameter distributions, not shown for brevity, exhibit a dominance of

20   relatively short MTTs in the hydrology of the Zhurucay basin. The CDFs also indicate that the

21   tracer is completely recovered in all catchments at around 80 biweeks, except for M7, where

22   the tracers is even more rapidly recovered (~ 19 biweeks). As we used a stable isotopic record

23   of 78 weeks (3 years), these results indicate that a three years record of tracer data is sufficient

24   to estimate the MTT of waters using the LCA in this páramo basin.

25   **3.4   Correlations of baseflow MTT with landscape and hydrometric variables**

26   Correlation analysis showed no statistically significant correlations (p-values > 0.05) between

27   MTT and landscape features and hydrometric variables of the nested monitoring system when

28   all catchments were included. This lack of correlation is likely related to the previously

29   reported distinct responsiveness of catchment M7 to precipitation inputs due to its different

16

1 geomorphologic configuration (i.e., ponded eutrophic wetland disconnected from the slopes)

2 and catchments M3 and M4 (Figure 1) driven by a spring water contribution during low flow

3 generation. In general, deep subsurface flow and groundwater contributions to discharge seem

4 to be minimal and geology has not been found to directly control the hydrology in this páramo

5 ecosystem (Mosquera et al., 2015). However, the existence of this shallow spring sourced at

6 the interface between the soil mineral horizon and the shallow bedrock upstream the outlet of

7 M3 and M4, favors the generation of higher low flows (Mosquera et al., 2016) and increases

8 MTTs in these catchments. The latter indicates that geology (fractures in the shallow bedrock)

9 influence the hydrology of these small headwater catchments; thus, masking relationships

10 between landscape features and MTT of the whole system. Therefore, we tested the MTT

11 correlations without including these small catchments (M3 and M4) and M7.

12 The reanalysis with the modified data set revealed significant relations of MTT with

13 topographical indexes (Figure 6). The relations between MTT and average slope (Figure 6a,

14 $R^2 = 0.78$ and p = 0.047) and percent area having slopes in the range 20%-40% are negative

15 (Figure 6b, $R^2 = 0.90$, p = 0.015). Conversely the relation between the percent area having

16 slopes 0%-20% and MTT is positive ($R^2 = 0.85$, p = 0.026). No significant correlations (p-

17 values > 0.05) between MTT and vegetation, soil types, geology, flow path length,

18 topographic wetness index, and hydrometric variables were found (Table 7). However, a

19 relatively strong relation between MTTs and low flows with smaller significance was also

20 found. That is, catchments with higher MTTs yielded lower low flows ($R^2 = 0.62$, p = 0.11 for

21 Q_5 and $R^2 = 0.61$, p = 0.12 for Q_{10}). The regression analysis including all catchments also

22 showed that mean electrical conductivity (MEC) of the waters explains 89% (p = < 0.001) of

23 the catchments' MTT variability (Figure 7). Streams with higher MEC have longer MTTs.

24 **4   Discussion**

25 **4.1   General hydrometric and isotopic characterization**

26 The rainfall-runoff process evidences a rapid response of discharge to precipitation inputs in

27 the Zhurucay basin. This rapid response occurs even during the less humid periods (August-

28 September) in which relatively small rainfall events result in peak flow generation (Figure

29 2a). This high responsiveness results from the combined effect of the relatively uniform

17

1 distribution of precipitation year-round – common in tropical regions – and the unique

2 properties of the Histosol soils or Andean wetlands located near the streams. The high storage

3 capacity of wetlands was also highlighted by (Roa-García and Weiler, 2010) after the

4 comparison of three paired catchments in the growing coffee region of Colombia at lower

5 elevations (2000-2200 m a.s.l.). Similarly, Histosol soils in our study site are rich in organic

6 matter content (mean 86% by volume), allowing for high water storage capacity. In addition,

7 due to their relatively low saturated hydraulic conductivity (0.72-1.55 cm h^{-1}), these soils

8 remain near saturation throughout the year. These factors, in combination with the local

9 climate, allow páramo soils to regulate and maintain a sustained discharge throughout the

10 year. Moreover, as these processes occur in the shallow organic horizon of the soils, the

11 hydrology of the Zhurucay basin páramo ecosystem is dominated by shallow subsurface water

12 flow. This is supported by the similar isotopic composition between streams and soil waters in

13 the organic layer of the Histosols in the Zhurucay basin (Mosquera et al., 2016).

14 Although the δ^{18}O isotopic composition of stream waters is damped and lagged with respect

15 to that of precipitation, streamflow samples in the Zhurucay basin still reflect the variability

16 of the δ^{18}O composition of rainfall (Figure 2b), as expected in a system dominated by shallow

17 subsurface flow. However, catchments are differently influenced by precipitation. M7, located

18 at the outlet of a wetland that remains constantly ponded, shows a faster response to rainfall

19 (Figure 5c), most likely as a result of the rapid mixing of rainfall water with the shallow water

20 moving in the shallow organic horizon of the soils and the ponded water above it. All of the

21 other catchments show considerably less influence of rainfall (Figures 5a and 5b) due to the

22 mixing of rainfall water with the water stored within the whole profile of the Histosol soils.

4.2 What is the baseflow MTT?

24 The high performance (KGE > 0.48) of the exponential model (EM) and its strong parameter

25 identifiability (Table 6) indicate that this model best mimics the subsurface transport of water

26 in all catchments within the Zhurucay basin (Figure 5). In addition, the model captures some

27 particularities in the functioning of each catchment. For instance, results indicate relatively

28 long MTTs in two of the headwater catchments, M3 and M4 (0.73 and 0.67 years,

29 respectively). This likely results from a shallow spring water contribution to these catchments

1 during low flow generation (Mosquera et al., 2015). The model seems to capture the effect of

2 the shallow spring contribution by yielding the longest MTTs estimations in these catchments,

3 and an intrinsic influence of geology on MTT variability. In addition, the performance of the

4 model in these two catchments is the lowest within the basin. The latter most likely because

5 of less efficient mixing of water due to the influence of the spring water source; suggesting

6 that this effect is also captured by the model which assumes a well-mixed reservoir. This

7 observation led us to consider that another model representing an additional slow reservoir

8 (e.g., TPLR or GM) might better represent the subsurface movement of water in these

9 catchments. Results, however, (Figures 3 and 4, Table 5) indicate that the contribution from

10 this additional water source is small and an additional reservoir is not well distinguished by

11 these TTDs as their parameters are not well identified. Recently, Muñoz-Villers et al. (2015)

12 also identified the EM as the model that best mimics subsurface flow in 7 of 12 nested

13 catchments underlain by volcanic soils (Andosols) in a tropical montane cloud forest (TMCF)

14 located in Veracruz, Mexico. These authors estimated even longer MTTs (1.2-2.2 years) due

15 to deeper groundwater contributions to discharge.

16 On the other end, M7, dominated by contribution from the shallowest part of the organic

17 horizon of the soils and the ponded fraction of water accumulated in a ponded wetland –

18 which is directly connected to the stream channel – presents the shortest MTT of all

19 catchments (0.15 years, 53 days), linked to the highest model performance. Our results

20 support the hypothesis that this catchment presents a shorter MTT, indicating that the ponded

21 condition of the wetland allows for a rapid and efficient mixture of precipitated water with

22 ponded water and water stored in and released from the shallow organic horizon of the soil.

23 The latter resulting in a rapid delivery of event (new) water to the stream; whereas water

24 stored deeper in the soil seems to remain mostly immobile with minimal influence in the

25 hydrology of the catchment. The well-mixing and simpler delivery of water to the stream is

26 also captured by the high model performance. The MTTs estimated for the rest of the

27 catchments lie in between these two extremes and their values and efficiencies vary

28 depending on the amplitude of the isotopic tracer variation, with longer MTTs in catchments

29 were the amplitude of the signal is more damped – evidencing lower influence of precipitation

30 and less efficient mixing with the soil storage – and vice versa. The MTT in these catchments

1 vary relatively little in comparison to the rest of the catchments (0.43 to 0.53 years, 156 to

2 191 days). Overall, the MTTs are relatively short, further supporting previous evidence that

3 shallow subsurface flow dominates the hydrology of the ecosystem.

4 In other tropical latitudes, MTTs higher than 300 days were found in three paired Colombian

5 catchments applying the TPLR model (Roa-García and Weiler, 2010). These basins show

6 higher MTTs than the catchments in the Zhurucay basin most likely as a result of the higher

7 development of the volcanic ash soils (> 10 m), which allow the water to be stored for longer

8 periods in the subsurface. MTTs longer than two years were also found in a TMCF in

9 southern Ecuador (Timbe et al., 2014), evidencing that differently from our findings, this

10 lower elevation ecosystem is dominated by deep groundwater contributions. Preliminary

11 MTT estimations in another TMCF biome located in central Mexico (Muñoz-Villers and

12 McDonnell, 2012) yielded a MTT of three years. Although the ecosystem is dominated by

13 soils formed by volcanic ash accumulation, as the páramo soils are, a combination of deeper

14 hillslope soils (1.5-3 m depth) with highly fractured and permeable geology allows for the

15 formation of longer flow paths of water and longer MTTs. Therefore, the relatively young and

16 little weathered geology in the Zhurucay basin allows for a dominance of shallow subsurface

17 flows. The results of these studies suggest that the particular shallow development of the rich

18 organic soils with low saturated hydraulic conductivities, in combination with an

19 homogeneous and low permeable geology provide the páramo basin of the Zhurucay River

20 with a high water retention capacity, and relatively long transit times and flow paths

21 considering the little development of the organic horizon of the soils. Hrachowitz et al.

22 (2009b) reported MTTs (135-202 days) around the ones found in the Zhurucay basin

23 catchments in a montane catchment in Scotland dominated by peatland soils and relatively

24 little weathering geology. Nevertheless, the models which provided the best fit were the GM

25 and the TPLR, as opposed to the EM in our study site. As in the Zhurucay basin, these authors

26 attributed this short transit time to the dominance of ecohydrological processes occurring in

27 the upper horizon of the peat soils. Therefore, we can conclude that in these two ecosystems,

28 located at different latitudes but with similar hydropedological conditions, the hydrology is

29 dominated by shallow subsurface flows. Nevertheless, the soils development of the shallow

30 peaty soils in Scotland is lower (40 cm) in comparison to the soil development of the

1 Histosols (80 cm) in the Zhurucay basin. These factors, in combination with differences

2 underlying geologies suggest that their overall hydrologic functioning might differ as

3 evidenced by different TTDs describing the subsurface transport of solutes.

4 Although we used a methodology that assumes stationary conditions in the hydrologic system

5 (LCA), it is relevant to note here the results of a recent application of conceptual modeling for

6 the investigation of non-stationary conditions in a hydrologically similar region (Birkel et al.,

7 2015). These authors detected non-stationary effects in water age distributions only during

8 extreme weather conditions (extensive dry or wet periods) and attributed this behavior to the

9 large mixing capacity of the Histosol soils. Although future investigations of the non-

10 stationary nature of MTTs are needed at the páramo, based on the dominance of flow

11 generation in the Histosols at the Zhurucay basin, in combination with low annual changes in

12 the environmental conditions, we consider our results from the LCA provide robust MTTs

13 estimates in our study site.

14 ## 4.3   Controls on baseflow MTT variability

15 We found significant correlations ($R^2 \geq 0.78$, $p < 0.05$) between catchment slope dependent

16 indexes and MTT using a subset of the main stream catchments (subgroup 2) (Table 7, Figure

17 6). Results of the correlation analysis indicate that 1) the higher the average slope of the

18 catchments, the shorter the MTT; 2) the higher the percent of area corresponding to slopes

19 between 0% and 20%, the longer the MTT; and 3) the higher the percent of area

20 corresponding to slopes between 20% and 40%, the shorter the MTT. These results indicate a

21 clear control of the catchments' slopes in the Zhurucay basin´s MTTs. Locally, the same

22 topographical features were found to control low flow generation. Mosquera et al. (2015)

23 attributed the latter to expected contributions from the water originated in the slopes (Andosol

24 soils) during low flow generation as a result of the gravitational potential of the water that

25 drains downslope from these soils. These authors also found that wetlands (Histosols soils

26 located near the streams) control the generation of moderate and high flows. Although we did

27 not find significant correlations with other landscape features, vegetation shown expected

28 trends in relation to MTT. That is, catchments with higher proportion of cushion plants

29 (wetlands) ($R^2 = 0.29$, $p = 0.35$) have longer MTTs and an inverse relation with tussock grass

1   vegetation ($R^2 = 0.31$, p = 0.33). In another tropical system of catchments in Colombia, a

2   catchment with higher areal proportion of wetlands was found to prolong the water MTTs, but

3   appeared to reduce water yield (Roa-García et al., 2011). Although these authors did not

4   report the slope of the catchments, we can infer that the catchment with the highest proportion

5   of wetlands – as they form in flat areas – is also the catchment with the lowest gradients.

6   Therefore, their observations might result from the combination of the deeper soil

7   development (> 10 m) with high water retention capacity and low saturated hydraulic

8   conductivity, perhaps in combination with low slope gradients. This would support the result

9   of our study, where the catchments with the lower slopes and higher proportion of wetlands

10   present the longer MTTs.

11   In other latitudes, in 20 Scottish catchments with different geomorphologies and climate,

12   MTT variability was controlled by the areal proportion of peat soils and no influence of

13   catchments' slopes was found (Hrachowitz et al., 2009a). As such, and given the similarities

14   between these soils and our Histosol soils (Andean wetlands), we hypothesized MTT

15   variability to be controlled by the areal extent of wetlands. Even though we found that MTT

16   variability is rather mainly controlled by topography in our tropical alpine site, a small trend

17   of wetlands' cover to increase MTT was also identified. Although the later relation is not

18   statistically significant, the latter most likely results from the influence of topography on

19   Histosol soils (wetlands) formation, where the formation of this soil mainly occurs in

20   catchments with lower slopes where water accumulation is favored. This finding indirectly

21   suggests that wetlands influence MTT spatial variability to a lesser extent. Therefore, it

22   appears that although relatively similar processes control the ecohydrology of both

23   ecosystems, controls on MTT variability cannot be extended from one ecosystem to the other.

24   MTT variability was also found to be controlled by the proportion of wetlands in cold snow

25   dominate boreal catchments in Sweden for the MTT of spring snowmelt water (Lyon et al.,

26   2010). These authors attributed this effect to the formation of shallow ice acting as

27   impermeable barriers above the wetlands, and thus changing the flow paths of water.

28   Nevertheless, because of the different climate and geological features between their

29   catchments and ours, we did not find wetlands as major controls on MTT variability.

1 Other slope topographic indexes – e.g., flow path length (L), flow path gradient (G), and the

2 ratio between both (L/G) (e.g., McGuire et al., 2005; Tetzlaff et al., 2009) – have been

3 identified as controls of MTT variability in catchments in other latitudes. Although these

4 landscape features did not significantly explain MTT variability in the Zhurucay basin, the

5 L/G ratio was reported as the major control of MTT variability ($R^2 = 0.91$) in steep temperate

6 catchments in the central western Cascades of Oregon (McGuire et al., 2005), suggesting that

7 this relation "reflects the hydraulic driving force of catchment-scale transport (i.e., Darcy's

8 law)". Similarly to our study site, they also found average slope of these catchments to be one

9 of the most important individual controls on MTT, explaining 78% of the MTT variability.

10 Recently, topography was also identified as a major control on the MTT of 12 TMCF

11 catchments in eastern Mexico (Muñoz-Villers et al., 2015). Results from these studies reflect

12 that the integrated effect of catchment slope on MTT variation can be identified in distinct

13 geological and hydropedological provinces. The latter also suggests that rather than using a

14 predictor which indicates more local effects of hydraulic force driving in the stream channel

15 (e.g., L/G), catchment slope might be a better measure to compare catchment functioning as it

16 integrates the hydrologic connectivity of hillslope, riparian, and stream areas.

17 The topographic controls on MTT in the Zhurucay basin indicate that water resides for a

18 longer time in catchments having lower slope gradients. These results also indicate that in

19 catchments having higher areal proportions of low gradients and lower areal proportions of

20 steeper gradients coupled with higher wetlands coverage, water resides longer in the shallow

21 reservoir of the soils. The control of the proportion of steeper gradients in MTT variability

22 suggests that the gravitational potential of water draining downslope in the Andosol soils also

23 indirectly influences MTTs. Therefore, it is our interpretation that the hydrology of this

24 ecosystem is mainly dominated by the interplay of two factors: 1) the high storage capacity in

25 the shallow organic horizon of the porous páramo soils and 2) the catchment slope. Factor 1

26 driving the high water retention capacity and factor 2 controlling the high regulation capacity

27 of the ecosystem, and thus, maintaining a sustained delivery of water to the streams along the

28 year. Without the interplay storage-slope, water would remain stored in the soils, and perhaps

29 the delivery of water towards the streams would be dominated by saturated overland flow

1 (SOF), affecting the regulation capacity of the ecosystem. Nevertheless, SOF rarely occurs in

2 the Zhurucay basin (Mosquera et al., 2015).

3 Mean electrical conductivity (MEC) was also found to be significantly correlated with MTT

4 using all catchments of the nested system in the basin (Figure 7). The regression analysis,

5 showed strong correlation, with MEC increasing as MTT increases. As EC is an intrinsic

6 property of water, due to the time it spends in contact with the surrounding pore space, rather

7 than a control on MTT variability, this result indicates that this property might be used as a

8 proxy to estimate MTT spatial variability. The well-defined connection between MTT and

9 MEC most likely resulting from the relatively homogenous geology of the Zhurucay basin. To

10 our knowledge, there are no studies that have identified similar (or different) relations

11 between MEC and MTT in other biomes.

12 Given that estimating MTT using isotope tracers and the LCA is financially expensive due to

13 the logistical set up of a monitoring network and the processes of data collection and analysis,

14 finding proxies (i.e., predictors) which allow inferring MTTs at lower operational costs is

15 critical to improve water resources management. In this sense, the strong relation between

16 MEC and MTT indicates that MEC could be used as a relatively inexpensive and directly

17 measurable proxy for MTT in this wet Andean páramo catchment. Therefore, although this

18 result cannot be expanded beyond páramo areas, perhaps not even beyond the study site, it

19 seems that it is worth evaluating whether or not MEC can infer MTT in other hydrologic

20 systems. Nevertheless, one should be careful that EC measurements can be relatively variable

21 over time. As a result, a single measurement of EC is most likely not enough to provide

22 robust MTT estimates. Therefore, longer EC measurement records reduce MEC variability

23 and provide more robust MTT estimates.

24 **5   Conclusions**

25 The baseflow MTT evaluation using a LCA indicated that the EM best describes the

26 subsurface transport of water in the basin. This result indicates efficient mixing in the high

27 organic and porous wet Andean páramo soils and a simple subsurface transition of rainfall

28 water towards the streams. MTT estimations showed relatively short MTTs linked to

29 relatively short subsurface flow paths. Therefore, we confirm that the hydrologic system of

1   the tropical alpine biome of the Zhurucay basin is dominated by shallow subsurface flow.

2   MTT estimations showed that catchment M7, located at a flat hilltop at the outlet of a wetland

3   which remains ponded year-round and disconnected from the slopes – most likely as a result

4   of the eutrophication of a lagoon – showed a particularly low MTT (0.15 yr – 53 days) in

5   relation to the MTT in all of the other catchments (0.40-73 yr, 156-250 days) in which the

6   morphology corresponds to U-shaped valleys, with the wetlands located at the valley bottoms

7   near the streams and connected to the slopes. Two headwater catchments, M3 and M4,

8   showed the longest MTT, related to a small contribution from a spring shallowly sourced.

9   These results indicate that in this páramo ecosystem, the geomorphology of the wetlands and

10 geology to a lesser extent, influence the responsiveness of the streams to precipitation inputs.

11 Correlation analysis between landscape variables and MTT indicates that MTT variability is

12 mainly explained by the slope of the catchments, and a related influence of vegetation to a

13 lesser extent. Catchments with the steepest average slopes and lower proportion of wetlands

14 have the shortest MTTs. The lack of significant correlations between the MTTs and

15 hydrological response variables (runoff coefficient and specific discharge rates) indicate that

16 neither water yield, nor streamflow rates control the time water resides in subsurface of the

17 páramo soils. These results indicate that the interplay between the high storage capacity of the

18 páramo soils and the slope of the catchments define the ecosystem's high regulation capacity.

19 Mean electrical conductivity (MEC) of stream waters – with the oldest waters presenting the

20 highest MECs – seems to be a promising proxy of MTT in system of catchments under

21 homogeneous geological conditions. Finally, we want to highlight the usefulness of a nested

22 monitoring system for acquiring better process-based hydrologic functioning understanding.

23 For instance, if M3, M4, and/or M7 catchments would not have been monitored, the influence

24 of geology and/or geomorphology on catchment hydrological response could not have been

25 identified and important information about the whole ecosystem functioning would remain

26 unknown.

6

References

Akaike, H.: A new look at the statistical model identification, IEEE Trans. Automat. Contr., 19(6), 716–723, doi:10.1109/TAC.1974.1100705, 1974.

Amin, I. E. and Campana, M. E.: A general lumped parameter model for the interpretation of tracer data and transit time calculation in hydrologic systems, J. Hydrol., 179(1-4), 1–21, doi:10.1016/0022-1694(95)02880-3, 1996.

Bethke, C. M. and Johnson, T. M.: Paradox of groundwater age: Correction, Geology, 30(4), 385–388, doi:10.1130/0091-7613(2002)030, 2002.

Beven, K. and Binley, A.: The future of distributed models: Model calibration and uncertainty prediction, Hydrol. Process., 6(3), 279–298, doi:10.1002/hyp.3360060305, 1992.

Beven, K. and Freer, J.: Equifinality, data assimilation, and uncertainty estimation in mechanistic modelling of complex environmental systems using the GLUE methodology, J. Hydrol., 249(1-4), 11–29, doi:10.1016/S0022-1694(01)00421-8, 2001.

Beven, K. and Kirkby, M.: A Physically Based, Variable Contributing Area Model of Basin Hydrology, Hydrol. Sci. Bull. Vol. 24, No. 1, p 43-69, March 1979. 16 fig, 1 tab, 36 ref, 24(1), 1979a.

Beven, K. J. and Kirkby, M. J.: A physically based, variable contributing area model of basin hydrology, Hydrol. Sci. Bull., 24(1), 43–69, doi:10.1080/02626667909491834, 1979b.

De Bièvre, B. and Calle, T.: Mountain Forum Bulletin 2011: Mountains and Green Economy. The Andean Páramo Project: Conserving biodiversity and hydrological services on the roof of the Andes., 2011.

Birkel, C., Soulsby, C. and Tetzlaff, D.: Conceptual modelling to assess how the interplay of hydrological connectivity, catchment storage and tracer dynamics controls nonstationary water age estimates, Hydrol. Process., 29(13), 2956–2969, doi:10.1002/hyp.10414, 2015.

Broxton, P. D., Troch, P. A. and Lyon, S. W.: On the role of aspect to quantify water transit times in small mountainous catchments, Water Resour. Res., 45(8), n/a–n/a, doi:10.1029/2008WR007438, 2009.

Buytaert, W. and Beven, K.: Models as multiple working hypotheses: hydrological simulation of tropical alpine wetlands, Hydrol. Process., 25(11), 1784–1799, doi:10.1002/hyp.7936, 2011.

1 Buytaert, W., Célleri, R., De Bièvre, B., Cisneros, F., Wyseure, G., Deckers, J. and Hofstede,

2 R.: Human impact on the hydrology of the Andean páramos, Earth-Science Rev., 79(1-2), 53–

3 72, doi:10.1016/j.earscirev.2006.06.002, 2006.

4 Célleri, R. and Feyen, J.: The Hydrology of Tropical Andean Ecosystems: Importance,

5 Knowledge Status, and Perspectives, Mt. Res. Dev., 29(4), 350–355, doi:10.1659/mrd.00007,

6 2009.

7 Coltorti, M. and Ollier, C. .: Geomorphic and tectonic evolution of the Ecuadorian Andes,

8 Geomorphology, 32(1-2), 1–19, doi:10.1016/S0169-555X(99)00036-7, 2000.

9 Córdova, M., Carrillo-Rojas, G., Crespo, P., Wilcox, B. and Célleri, R.: Evaluation of the

10 Penman-Monteith (FAO 56 PM) Method for Calculating Reference Evapotranspiration Using

11 Limited Data, Mt. Res. Dev., 35(3), 230–239, doi:10.1659/MRD-JOURNAL-D-14-0024.1,

12 2015.

13 Craig, H.: Standard for Reporting Concentrations of Deuterium and Oxygen-18 in Natural

14 Waters., Science, 133(3467), 1833–4, doi:10.1126/science.133.3467.1833, 1961.

15 Crespo, P., Bücker, A., Feyen, J., Vaché, K. B., Frede, H.-G. and Breuer, L.: Preliminary

16 evaluation of the runoff processes in a remote montane cloud forest basin using Mixing Model

17 Analysis and Mean Transit Time, Hydrol. Process., 26(25), 3896–3910, doi:10.1002/hyp.8382,

18 2012.

19 Crespo, P. J., Feyen, J., Buytaert, W., Bücker, A., Breuer, L., Frede, H.-G. and Ramírez, M.:

20 Identifying controls of the rainfall–runoff response of small catchments in the tropical Andes

21 (Ecuador), J. Hydrol., 407(1-4), 164–174, doi:10.1016/j.jhydrol.2011.07.021, 2011.

22 Davies, J., Beven, K., Rodhe, A., Nyberg, L. and Bishop, K.: Integrated modeling of flow and

23 residence times at the catchment scale with multiple interacting pathways, Water Resour. Res.,

24 49(8), 4738–4750, doi:10.1002/wrcr.20377, 2013.

25 Duvert, C., Stewart, M. K., Cendón, D. I. and Raiber, M.: Time series of tritium, stable isotopes

26 and chloride reveal short-term variations in groundwater contribution to a stream, Hydrol. Earth

27 Syst. Sci., 20(1), 257–277, doi:10.5194/hess-20-257-2016, 2016.

28 Etcheverry, D. and Perrochet, P.: Direct simulation of groundwater transit-time distributions

29 using the reservoir theory, Hydrogeol. J., 8(2), 200–208, doi:10.1007/s100400050006, 2000.

Farrick, K. K. and Branfireun, B. A.: Flowpaths, source water contributions and water residence times in a Mexican tropical dry forest catchment, J. Hydrol., 529, 854–865, doi:10.1016/j.jhydrol.2015.08.059, 2015.

Freeze, R. A.: Role of subsurface flow in generating surface runoff: 2. Upstream source areas, Water Resour. Res., 8(5), 1272–1283, doi:10.1029/WR008i005p01272, 1972.

Goldsmith, G. R., Muñoz-Villers, L. E., Holwerda, F., McDonnell, J. J., Asbjornsen, H. and Dawson, T. E.: Stable isotopes reveal linkages among ecohydrological processes in a seasonally dry tropical montane cloud forest, Ecohydrology, 5(6), 779–790, doi:10.1002/eco.268, 2012.

Goller, R., Wilcke, W., Leng, M. J., Tobschall, H. J., Wagner, K., Valarezo, C. and Zech, W.: Tracing water paths through small catchments under a tropical montane rain forest in south Ecuador by an oxygen isotope approach, J. Hydrol., 308(1-4), 67–80, doi:10.1016/j.jhydrol.2004.10.022, 2005.

Gupta, H. V., Kling, H., Yilmaz, K. K. and Martinez, G. F.: Decomposition of the mean squared error and NSE performance criteria: Implications for improving hydrological modelling, J. Hydrol., 377(1-2), 80–91, doi:10.1016/j.jhydrol.2009.08.003, 2009.

Hale, V. C. and McDonnell, J. J.: Effect of bedrock permeability on stream base flow mean transit time scaling relations: 1. A multiscale catchment intercomparison, Water Resour. Res., n/a–n/a, doi:10.1002/2014WR016124, 2016.

Hale, V. C., McDonnell, J. J., Stewart, M. K., Solomon, D. K., Doolitte, J., Ice, G. G. and Pack, R. T.: Effect of bedrock permeability on stream base flow mean transit time scaling relationships: 2. Process study of storage and release, Water Resour. Res., n/a–n/a, doi:10.1002/2015WR017660, 2016.

Harman, C. J.: Time-variable transit time distributions and transport: Theory and application to storage-dependent transport of chloride in a watershed, Water Resour. Res., 51(1), 1–30, doi:10.1002/2014WR015707, 2015.

Heidbüchel, I., Troch, P. A., Lyon, S. W. and Weiler, M.: The master transit time distribution of variable flow systems, Water Resour. Res., 48(6), W06520, doi:10.1029/2011WR011293, 2012.

Hewlett, J. D.: Soil moisture as a source of base flow from steep mountain watersheds, U.S.

Dept of Agriculture, Forest Service, Southeastern Forest Experiment Station, Asheville, N.C., 1961.

Hrachowitz, M., Soulsby, C., Tetzlaff, D., Dawson, J. J. C. and Malcolm, I. A.: Regionalization of transit time estimates in montane catchments by integrating landscape controls, Water Resour. Res., 45(5), n/a–n/a, doi:10.1029/2008WR007496, 2009a.

Hrachowitz, M., Soulsby, C., Tetzlaff, D., Dawson, J. J. C., Dunn, S. M. and Malcolm, I. A.: Using long-term data sets to understand transit times in contrasting headwater catchments, J. Hydrol., 367(3-4), 237–248, doi:10.1016/j.jhydrol.2009.01.001, 2009b.

Hrachowitz, M., Soulsby, C., Tetzlaff, D., Malcolm, I. A. and Schoups, G.: Gamma distribution models for transit time estimation in catchments: Physical interpretation of parameters and implications for time-variant transit time assessment, Water Resour. Res., 46(10), n/a–n/a, doi:10.1029/2010WR009148, 2010.

Hrachowitz, M., Soulsby, C., Tetzlaff, D. and Malcolm, I. A.: Sensitivity of mean transit time estimates to model conditioning and data availability, Hydrol. Process., 25(6), 980–990, doi:10.1002/hyp.7922, 2011.

Hrachowitz, M., Savenije, H., Bogaard, T. A., Tetzlaff, D. and Soulsby, C.: What can flux tracking teach us about water age distribution patterns and their temporal dynamics?, Hydrol. Earth Syst. Sci., 17(2), 533–564, doi:10.5194/hess-17-533-2013, 2013.

Hu, K., Chen, H., Nie, Y. and Wang, K.: Seasonal recharge and mean residence times of soil and epikarst water in a small karst catchment of southwest China., Sci. Rep., 5, 10215, doi:10.1038/srep10215, 2015.

IUCN: High Andean Wetlands, Gland, Switzerland., 2002.

Kirchner, J. W.: Aggregation in environmental systems – Part 1: Seasonal tracer cycles quantify young water fractions, but not mean transit times, in spatially heterogeneous catchments, Hydrol. Earth Syst. Sci., 20(1), 279–297, doi:10.5194/hess-20-279-2016, 2016a.

Kirchner, J. W.: Aggregation in environmental systems – Part 2: Catchment mean transit times and young water fractions under hydrologic nonstationarity, Hydrol. Earth Syst. Sci., 20(1), 299–328, doi:10.5194/hess-20-299-2016, 2016b.

Kirchner, J. W., Feng, X. and Neal, C.: Fractal stream chemistry and its implications for

contaminant transportin catchments, Nature, 403(6769), 524–527, doi:10.1038/35000537, 2000.

Klaus, J., Chun, K. P., McGuire, K. J. and McDonnell, J. J.: Temporal dynamics of catchment transit times from stable isotope data, Water Resour. Res., 51(6), 4208–4223, doi:10.1002/2014WR016247, 2015.

Kreft, A. and Zuber, A.: On the physical meaning of the dispersion equation and its solutions for different initial and boundary conditions, Chem. Eng. Sci., 33(11), 1471–1480, doi:10.1016/0009-2509(78)85196-3, 1978.

Lyon, S. W., Laudon, H., Seibert, J., Mörth, M., Tetzlaff, D. and Bishop, K. H.: Controls on snowmelt water mean transit times in northern boreal catchments, Hydrol. Process., 24(12), 1672–1684, doi:10.1002/hyp.7577, 2010.

Maloszewski, P. and Zuber, A.: Lumped parameter models for the interpretation of environmental tracer data, in Manual on Mathematical Models in Isotope Hydrogeology. TECDOC-910., 1996.

Małoszewski, P. and Zuber, A.: Determining the turnover time of groundwater systems with the aid of environmental tracers, J. Hydrol., 57(3-4), 207–231, doi:10.1016/0022-1694(82)90147-0, 1982.

McDonnell, J. J., McGuire, K., Aggarwal, P., Beven, K. J., Biondi, D., Destouni, G., Dunn, S., James, A., Kirchner, J., Kraft, P., Lyon, S., Maloszewski, P., Newman, B., Pfister, L., Rinaldo, A., Rodhe, A., Sayama, T., Seibert, J., Solomon, K., Soulsby, C., Stewart, M., Tetzlaff, D., Tobin, C., Troch, P., Weiler, M., Western, A., Wörman, A. and Wrede, S.: How old is streamwater? Open questions in catchment transit time conceptualization, modelling and analysis, Hydrol. Process., 24(12), 1745–1754, doi:10.1002/hyp.7796, 2010.

McGlynn, B. L. and McDonnell, J. J.: Quantifying the relative contributions of riparian and hillslope zones to catchment runoff, Water Resour. Res., 39(11), n/a–n/a, doi:10.1029/2003WR002091, 2003.

McGuire, K. ., DeWalle, D. . and Gburek, W. .: Evaluation of mean residence time in subsurface waters using oxygen-18 fluctuations during drought conditions in the mid-Appalachians, J. Hydrol., 261(1-4), 132–149, doi:10.1016/S0022-1694(02)00006-9, 2002.

McGuire, K. J. and McDonnell, J. J.: A review and evaluation of catchment transit time modeling, J. Hydrol., 330(3-4), 543–563, doi:10.1016/j.jhydrol.2006.04.020, 2006.

McGuire, K. J., McDonnell, J. J., Weiler, M., Kendall, C., McGlynn, B. L., Welker, J. M. and Seibert, J.: The role of topography on catchment-scale water residence time, Water Resour. Res., 41(5), n/a–n/a, doi:10.1029/2004WR003657, 2005.

McMillan, H., Tetzlaff, D., Clark, M. and Soulsby, C.: Do time-variable tracers aid the evaluation of hydrological model structure? A multimodel approach, Water Resour. Res., 48(5), n/a–n/a, doi:10.1029/2011WR011688, 2012.

Mook, W. G.: Introduction: Theory , methods, review, in Environmental Isotopes in the Hydrological Cycle: Principles and Applications, edited by W. G. Mook, IAEA and UNESCO, Paris / Vienna., 2000.

Moore, R. D.: Introduction to salt dilution gauging for streamflow measurement Part 2: Constant-rate injection, Streamline Watershed Manag. Bull., 8(1), 11–15, 2004.

Mosquera, G. M., Lazo, P. X., Célleri, R., Wilcox, B. P. and Crespo, P.: Runoff from tropical alpine grasslands increases with areal extent of wetlands, CATENA, 125, 120–128, doi:10.1016/j.catena.2014.10.010, 2015.

Mosquera, G. M., Célleri, R., Lazo, P. X., Vaché, K. B. and Crespo, P. J.: Combined Use of Isotopic and Hydrometric Data to Conceptualize Ecohydrological Processes in a High-Elevation Tropical Ecosystem, Hydrol. Process., 2016.

Muñoz-Villers, L. E. and McDonnell, J. J.: Runoff generation in a steep, tropical montane cloud forest catchment on permeable volcanic substrate, Water Resour. Res., 48(9), n/a–n/a, doi:10.1029/2011WR011316, 2012.

Muñoz-Villers, L. E., Geissert, D. R., Holwerda, F. and McDonnell, J. J.: Factors influencing stream water transit times in tropical montane watersheds, Hydrol. Earth Syst. Sci. Discuss., 12(10), 10975–11011, doi:10.5194/hessd-12-10975-2015, 2015.

Padrón, R. S., Wilcox, B. P., Crespo, P. and Célleri, R.: Rainfall in the Andean Páramo: New Insights from High-Resolution Monitoring in Southern Ecuador, J. Hydrometeorol., 16(3), 985–996, doi:10.1175/JHM-D-14-0135.1, 2015.

Penna, D., Tromp-van Meerveld, H. J., Gobbi, A., Borga, M. and Dalla Fontana, G.: The

influence of soil moisture on threshold runoff generation processes in an alpine headwater catchment, Hydrol. Earth Syst. Sci., 15(3), 689–702, doi:10.5194/hess-15-689-2011, 2011.

Pratt, W. T., Figueroa, J. F. and Flores, B. G.: Geology and Mineralization of the Area between 3 and 48S. Western Cordillera, Ecuador. Open File Report, WCr97r28. British Geological Survey., 1997.

Quichimbo, P., Tenorio, G., Borja, P., Cárdenas, I., Crespo, P. and Célleri, R.: Efectos sobre las propiedades físicas y químicas de los suelos por el cambio de la cobertura vegetal y uso del suelo: páramo de Quimsacocha al sur del Ecuador., Suelos Ecuatoriales, 42(2), 138–153, 2012.

Ramsay, P. M. and Oxley, E. R. B.: The growth form composition of plant communities in the ecuadorian páramos, Plant Ecol., 131(2), 173–192, doi:10.1023/A:1009796224479, 1997.

Roa-García, M. C. and Weiler, M.: Integrated response and transit time distributions of watersheds by combining hydrograph separation and long-term transit time modeling, Hydrol. Earth Syst. Sci., 14(8), 1537–1549, doi:10.5194/hess-14-1537-2010, 2010.

Roa-García, M. C., Brown, S., Schreier, H. and Lavkulich, L. M.: The role of land use and soils in regulating water flow in small headwater catchments of the Andes, Water Resour. Res., 47(5), W05510, doi:10.1029/2010WR009582, 2011.

Rodhe, A., Nyberg, L. and Bishop, K.: Transit Times for Water in a Small Till Catchment from a Step Shift in the Oxygen 18 Content of the Water Input, Water Resour. Res., 32(12), 3497–3511, doi:10.1029/95WR01806, 1996.

Seeger, S. and Weiler, M.: Reevaluation of transit time distributions, mean transit times and their relation to catchment topography, Hydrol. Earth Syst. Sci., 18(12), 4751–4771, doi:10.5194/hess-18-4751-2014, 2014.

Segura, C., James, A. L., Lazzati, D. and Roulet, N. T.: Scaling relationships for event water contributions and transit times in small-forested catchments in Eastern Quebec, Water Resour. Res., 48(7), n/a–n/a, doi:10.1029/2012WR011890, 2012.

Sklenar, P. and Jorgensen, P. M.: Distribution patterns of paramo plants in Ecuador, J. Biogeogr., 26(4), 681–691, doi:10.1046/j.1365-2699.1999.00324.x, 1999.

Soulsby, C., Tetzlaff, D., Rodgers, P., Dunn, S. and Waldron, S.: Runoff processes, stream water residence times and controlling landscape characteristics in a mesoscale catchment: An

initial evaluation, J. Hydrol., 325(1-4), 197–221, doi:10.1016/j.jhydrol.2005.10.024, 2006.

Tetzlaff, D., Seibert, J., McGuire, K. J., Laudon, H., Burns, D. A., Dunn, S. M. and Soulsby, C.: How does landscape structure influence catchment transit time across different geomorphic provinces?, Hydrol. Process., 23(6), 945–953, doi:10.1002/hyp.7240, 2009.

Tetzlaff, D., Carey, S. K., Laudon, H. and McGuire, K.: Catchment processes and heterogeneity at multiple scales-benchmarking observations, conceptualization and prediction, Hydrol. Process., 24(16), 2203–2208, doi:10.1002/hyp.7784, 2010.

Tetzlaff, D., Al-Rawas, G., Blöschl, G., Carey, S. K., Fan, Y., Hrachowitz, M., Kirnbauer, R., Jewitt, G., Laudon, H., McGuire, K. J., Sayama, T., Soulsby, C., Zehe, E. and Wagener, T.: Process realism: Flow paths and storage., in Runoff prediction in ungauged basins: Synthesis across processes, places and scales, edited by G. Blösch, M. Sivapalan, T. Wagener, A. Viglione, and H. Savenije, pp. 53–69, Cambridge University Press, Cambridge, UK., 2013.

Tetzlaff, D., Birkel, C., Dick, J., Geris, J. and Soulsby, C.: Storage dynamics in hydropedological units control hillslope connectivity, runoff generation, and the evolution of catchment transit time distributions., Water Resour. Res., 50(2), 969–985, doi:10.1002/2013WR014147, 2014.

Timbe, E., Windhorst, D., Crespo, P., Frede, H.-G., Feyen, J. and Breuer, L.: Understanding uncertainties when inferring mean transit times of water trough tracer-based lumped-parameter models in Andean tropical montane cloud forest catchments, Hydrol. Earth Syst. Sci., 18(4), 1503–1523, doi:10.5194/hess-18-1503-2014, 2014.

U.S. Bureau of Reclamation: Water Measurement Manual, Washington DC., 2001.

van der Velde, Y., Heidbüchel, I., Lyon, S. W., Nyberg, L., Rodhe, A., Bishop, K. and Troch, P. A.: Consequences of mixing assumptions for time-variable travel time distributions, Hydrol. Process., 29(16), 3460–3474, doi:10.1002/hyp.10372, 2015.

Vimeux, F., Tremoy, G., Risi, C. and Gallaire, R.: A strong control of the South American SeeSaw on the intra-seasonal variability of the isotopic composition of precipitation in the Bolivian Andes, Earth Planet. Sci. Lett., 307(1-2), 47–58 [online] Available from: http://www.documentation.ird.fr/hor/fdi:010053700 (Accessed 3 December 2015), 2011.

Weiler, M., McGlynn, B. L., McGuire, K. J. and McDonnell, J. J.: How does rainfall become

1   runoff? A combined tracer and runoff transfer function approach, Water Resour. Res., 39(11),

2   n/a–n/a, doi:10.1029/2003WR002331, 2003.

3   Windhorst, D., Waltz, T., Timbe, E., Frede, H.-G. and Breuer, L.: Impact of elevation and

4   weather patterns on the isotopic composition of precipitation in a tropical montane rainforest,

5   Hydrol. Earth Syst. Sci., 17(1), 409–419, doi:10.5194/hess-17-409-2013, 2013.

6

7

Table 1. Main landscape characteristics of the monitored catchments.

Catchment	Area (km²)	Altitude (m a.s.l)	Distribution of soil types[a] (%)			Vegetation cover[b] (%)				Topography[c] (%)				Geology[e] (%)			EC[f] (µS/cm)
			AN	HS	LP	TG	CP	QF	PF	AS	L[d]	G	TWI	Qm	Tu	Qd	
M1	0.20	3777 – 3900	85	13	2	85	15	0	0	14	0.9	1.9	9.6	100	0	0	35.7
M2	0.38	3770 – 3900	83	15	2	87	13	0	0	24	0.8	1.9	12.8	66	1	33	32.0
M3	0.38	3723 – 3850	80	16	3	78	18	4	0	19	1.0	2.0	9.4	59	41	0	62.4
M4	0.65	3715 – 3850	76	20	4	79	18	3	0	18	1.3	2.0	12.5	50	48	1	47.9
M5	1.40	3680 – 3900	78	20	2	78	17	0	4	20	2.5	1.9	11.8	70	1	30	37.0
M6	3.28	3676 – 3900	74	22	4	73	24	1	2	18	3.3	1.8	8.2	50	30	20	35.6
M7	1.22	3771 – 3830	37	59	4	35	65	0	0	12	0.4	1.7	10	87	0	13	15.3
M8	7.53	3505 – 3900	72	24	5	71	24	2	2	17	4.6	1.9	16.7	56	31	13	33.5

[a] AN = Andosol; HS = Histosol; LP = Leptosol

[b] TG = tussock grasses; CP = cushion plants; QF = *Polylepys forest*; PF = pine forest.

[c] AS = average slope, L = flow path length ; G = flow path gradient; TWI = topographic wetness index (Beven and Kirkby, 1979a).

[d] L units in km.

[e] Qm = Quimsacocha formation; Tu = Turi formation; Qd = Quaternary deposits.

[f] EC = mean electrical conductivity. Data collected weekly for a three years period (June 2012-June2015)

1

1   Table 1. Models considered to describe water mean transit time (MTT) in the study area and

2   their transit time distribution (TTD) functions, parameters, and range of initial parameters.

Model	Transit time distribution ($g(\tau)$)	Parameter(s) range
Exponential model (EM)	$\dfrac{1}{\tau}\exp\left(\dfrac{-t}{\tau}\right)$	$\tau\,[0-130]$
Exponential-piston model (EPM)	$\dfrac{\eta}{\tau}\exp\left(-\dfrac{t\cdot\eta}{\tau}+\eta-1\right)$ for $t\geq\tau\,(1-\eta^{-1}$	$\tau\,[0-130]$ $\eta\,[0.5-4]$
Dispersion model (DM)	$\left(\dfrac{4\pi D_p t}{\tau}\right)^{-1/2}t^{-1}\exp\left[-\left(1-\dfrac{t}{\tau}\right)^2\left(\dfrac{\tau}{4D_p t}\right)\right]$	$\tau\,[0-130]$ $D_p\,[0.5-4]$
Gamma model (GM)	$\dfrac{\tau^{\alpha-1}}{\beta^\alpha\Gamma(\alpha)}\exp^{-\tau/\beta}$	$\alpha\,[0.01-4]$ $\beta\,[0-500]$ $\tau=\alpha\cdot\beta$
Two parallel linear reservoir (TPLR)	$\dfrac{\varphi}{\tau_f}\exp\left(\dfrac{-t}{\tau_f}\right)+\dfrac{1-\varphi}{\tau_f}\exp\left(\dfrac{-t}{\tau_s}\right)$	$\tau_s\,[0-130]$ $\tau_f\,[0-15]$ $\varphi\,[0-1]$

3   τ = tracer's mean transit time (MTT) [biweeks]; η = parameter that indicates the percentage of

4   contribution of each flow type [-]; Dp = dispersion parameter [-]; α = shape parameter [-]; β =

5   scale parameter [-]; τ_f and τ_s = transit time of fast and slow flows in biweeks; φ = flow

6   partition parameter between fast and slow flow reservoirs [%]. [-] Indicates parameters are

7   unitless.

Table 3. Main hydrometric variables of the catchments.

Catchment	Precipitation (mm yr^{-1})	Total runoff (mm yr^{-1})	Runoff Coefficient[b]	Average specific discharge (l s^{-1} km^{-2})	Flow rates as frequency of non-exceedance (l s^{-1} km^{-2})						
					Q_{min}	Q_{10}	Q_{30}	Q_{50}	Q_{70}	Q_{90}	Q_{max}
M1	1300	729	0.56	23.1	0.7	2.7	6.6	14.3	26.4	50.1	1039.0
M2	1300	720	0.55	22.8	1.2	4.8	7.9	14.9	26.7	49.0	762.9
M3	1293	841	0.65	26.7	2.3	7.3	10.8	17.7	28.1	52.4	894.2
M4	1294	809	0.62	25.6	4.2	6.2	9.8	16.6	27.3	52.1	741.2
M5	1267	766	0.6	24.3	1.5	4.1	8.3	15.3	26.9	50.8	905.7
M6	1254	786	0.63	24.9	1.2	3.7	8.2	15.9	27.5	53.2	930.4
M7	1231	684	0.56	21.7	0.3	1.8	5.2	11.0	23.3	53.9	732.0
M8	1277	864	0.68	27.4	1.9	4.0	8.7	15.2	29.2	60.8	777.9

[a] Total runoff as a proportion of precipitation.

1

1 Table 4. Statistics of the δ^{18}O isotopic composition in precipitation and streamflow used as

2 input data for the MTT modeling.

Sampling Station	Altitude (m a.s.l.)	δ^{18}O (‰)				
		n[a]	Average	SE[b]	Max	Min
M1	3840	123	−10.6	0.06	−9.0	−12.6
M2	3840	124	−10.4	0.07	−8.8	−12.6
M3	3800	121	−10.7	0.05	−8.8	−12.1
M4	3800	122	−10.6	0.05	−8.7	−11.9
M5	3800	118	−10.5	0.06	−9.1	−12.8
M6	3780	121	−10.3	0.06	−8.9	−12.2
M7	3820	121	−8.9	0.15	−6.2	−13.9
M8	3700	118	−10.0	0.06	−8.3	−11.6
Upper Precip.	3779	137	−10.2	0.32	−1.2	−25.0
Middle Precip.	3700	134	−10.1	0.32	−2.7	−20.0

3 [a] n: number of samples collected.

4 [b] SE: Standard error.

Table 5. Statistical parameters of observed and modeled δ18O for the stream at the outlet of the basin (M8).

Model	Observed δ18O		Simulated δ18O						Model Parameters[b]		MI[c] (%)
	Mean (‰)	σ[a] (‰)	Mean (‰)	σ[a] (‰)	KGE[a] (-)	RMSE[a] (‰)	Bias (‰)	AIC[a] (-)			
EM	-10.05	0.45	-10.02	0.52	0.63	0.59	0.03	2.92	τ (days)	191 (166-224)	4
EPM			-10.02	0.52	0.63	0.59	0.03	4.92	τ (days)	120 (90-205)	7
									η (-)	0.63 (0.53-0.92)	11
DM			-9.95	0.64	0.50	0.72	0.10	5.39	τ (days)	666 (480-755)	17
									Dp (-)	3.99 (2.74-3.93)	38
GM			-10.02	0.45	0.75	0.47	0.03	4.58	τ (days)	392 (296-1478)	59
									α (-)	0.70 (0.51-0.76)	7
									β (-)	40 (26-108)	18
TPLR			-10.02	0.45	0.76	0.47	0.03	6.55	τf (days)	1664 (356-1738)	85
									τs (days)	45 (12-90)	31
									φ (-)	0.31 (0.10-0.48)	43

[a] σ = Standard deviation; KGE = Kling-Gupta Efficiency (Gupta et al., 2009), AIC = Akaike Information Criterion (Akaike, 1974). Statistical parameters of the simulated results correspond to the best-matching value of the objective function KGE.

[b] τ = tracer's mean transit time; η = parameter that indicates the ratio between the contribution of piston and exponential flow; Dp = dispersion parameter; α = shape parameter; β = scale parameter; τf and τs = transit time of fast and slow flows in biweeks; φ = flow partition parameter between fast and slow flow reservoirs. (-) = Dimensionless parameter. Uncertainty bounds (5-95 percentiles) of simulated parameters shown in parenthesis were estimated using the generalized likelihood uncertainty estimation (GLUE, Beven and Binley, 1992).

[c] MI = Measure of identification (Segura et al., 2012), i.e., ratio of behavioral parameter range to initial parameter range.

1

Table 6. Statistical parameters of observed and simulated $\delta^{18}O$ for all catchments using the exponential model (EM).

Catchment	Observed $\delta^{18}O$		Simulated $\delta^{18}O$			Simulated MTT[b]	
	Mean	σ^a	Mean	σ^a	KGE[a]		
	(‰)	(‰)	(‰)	(‰)	(-)	(years)	(days)
M1	−10.63	0.37	−10.51	0.44	0.48	0.54 (0.48 – 0.63)	194 (171 – 227)
M2	−10.46	0.53	−10.51	0.63	0.61	0.43 (0.38 – 0.51)	156 (137 – 183)
M3	−10.64	0.23	−10.51	0.26	0.48	0.73 (0.64 – 0.86)	264 (232 – 310)
M4	−10.63	0.27	−10.51	0.3	0.48	0.67 (0.59 – 0.78)	240 (212 – 280)
M5	−10.51	0.39	−10.51	0.46	0.53	0.52 (0.46 – 0.61)	188 (165 – 219)
M6	−10.37	0.42	−10.43	0.5	0.59	0.52 (0.46 – 0.61)	188 (164 – 220)
M7	−8.93	2.92	−10.02	2.93	0.84	0.15 (0.12 – 0.18)	53 (45 – 64)
M8	−10.05	0.45	−10.02	0.52	0.63	0.53 (0.46 – 0.62)	191 (167 – 224)

[a] σ = Standard deviation; KGE = Kling-Gupta Efficiency. Statistical parameters of the simulated results correspond to the best-matching value of the objective function KGE.

[b] Uncertainty bounds (5-95 percentiles) of the simulated mean transit time (MTT) shown in parenthesis were estimated using the generalized likelihood uncertainty estimation (GLUE).

1

Table 7. Coefficient of determination (R^2) between the mean transit time (MTT) and i) landscape features and ii) hydrological variables for each of the catchments. Catchments M3 and M4 (additional spring water source, see Figure 1) and M7 (at a flat hilltop disconnected from the hillslopes) are not included in the regressions; except for electrical conductivity, i.e., all catchments are considered (Figure 7).

Landscape features			Hydrologic variables		
Vegetation			*General features*		
Cushion plant	0.29	(0.35)	Runoff coefficient	0.25	(0.39)
Tussock grass	− 0.31	(0.33)	Total runoff	0.21	(0.44)
			Precipitation	− 0.17	(0.48)
Soil Type			Average specific discharge	0.21	(0.44)
Histosol	0.13	(0.56)			
Andosol	− 0.13	(0.55)	*Streamflow rates*		
			Q_{99}	0.42	(0.24)
Geologic formation			Q_{90}	0.18	(0.48)
Quimsacocha	0.04	(0.75)	Q_{80}	0.06	(0.68)
Turi	0.12	(0.57)	Q_{70}	0.09	(0.63)
Quaternary deposits	− 0.51	(0.18)	Q_{60}	0.06	(0.68)
			Q_{50}	0.01	(0.86)
Topographic features			Q_{40}	0.10	(0.61)
Average slope	**− 0.78**	**(0.05)**	Q_{30}	− 0.02	(0.82)
Slope 0%−20%	**0.85**	**(0.03)**	Q_{20}	− 0.14	(0.53)
Slope 20%−40%	**− 0.90**	**(0.01)**	Q_{10}	− 0.61	(0.12)
Area	0.13	(0.56)	Q_5	− 0.62	(0.11)
TWI	− 0.03	(0.79)			
Flow path length (L)	0.23	(0.42)	*Water intrinsic properties*		
Flow path gradient (G)	− 0.20	(0.45)	Electrical conductivity	**0.95**	**(< 0.001)**
L/G	0.23	(0.45)			

Signs indicate positive (no sign) or negative (−) correlation between parameters.

Values in bold are statistically significant to a 95% level of confidence ($p < 0.05$). Values in parenthesis are the p-values of the correlations.

[a] TWI = Topographic wetness index (Beven and Kirby, 1979).
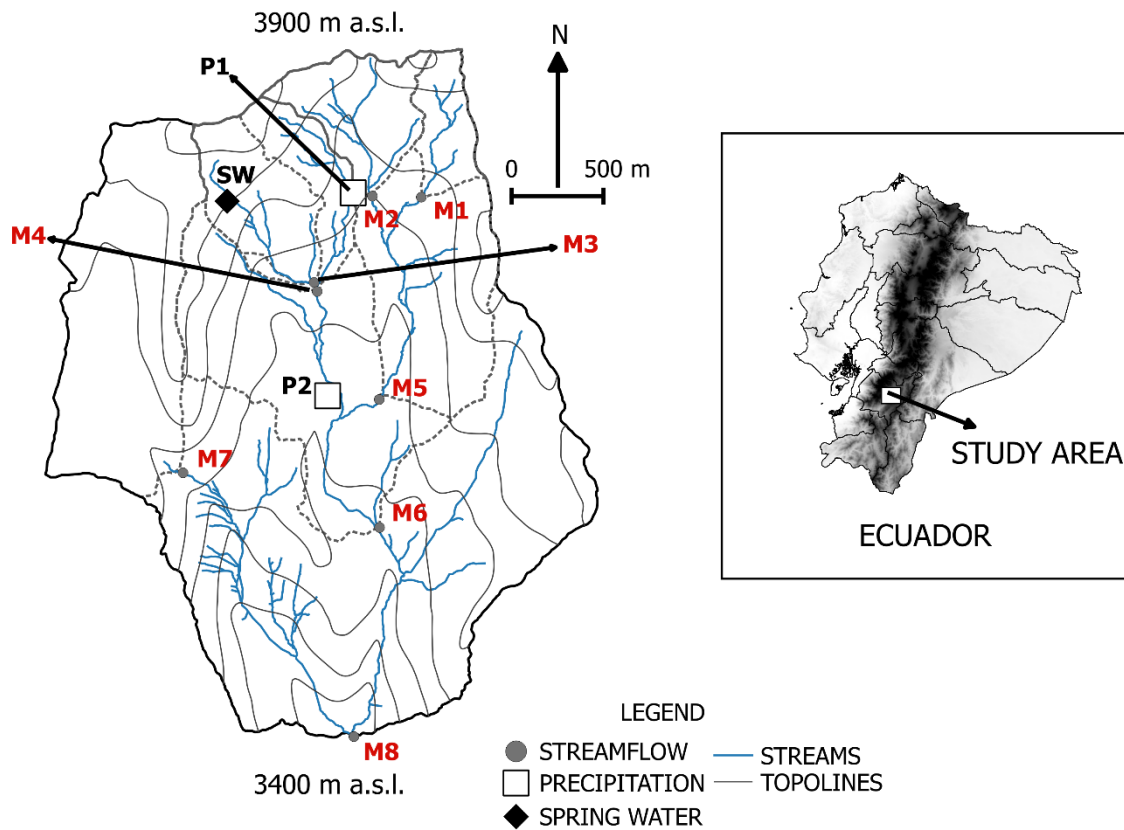
1

2   Figure 1. Location of the study area, and the isotopic monitoring stations in the Zhurucay

3   observatory for: Streamflow (M), and Precipitation (P). SW is a spring water source upstream

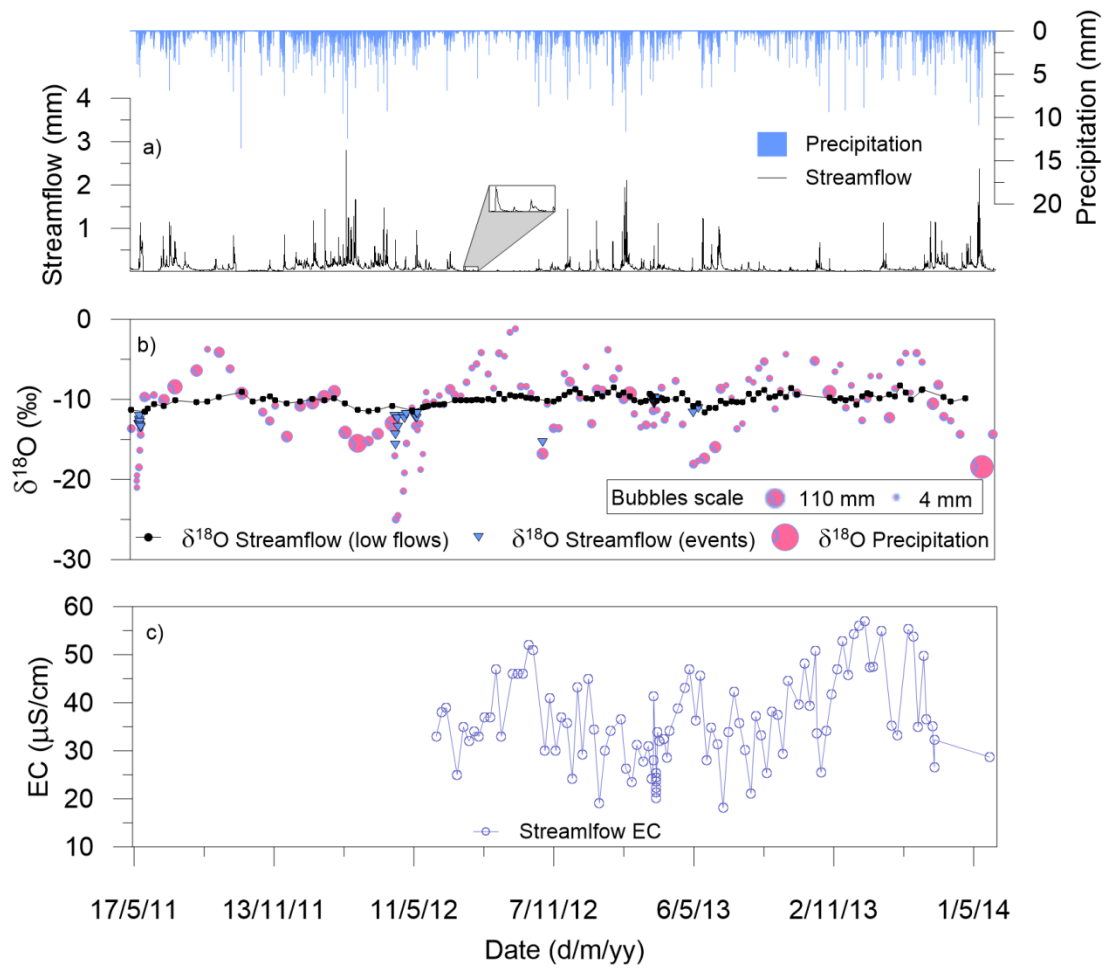4   the outlet of catchments M3 and M4.

Figure 2. a) Hourly precipitation and unit area streamflow; b) $\delta^{18}O$ isotopic composition in precipitation and streamflow for 3 years (May 2011-May 2014); and c) electrical conductivity for 2 years (May 2012-May 2014) at the catchment outlet (M8, see location in Figure 2). The size of the bubbles in plot b) indicates the relative cumulative rainfall in millimeters for each collected sample.
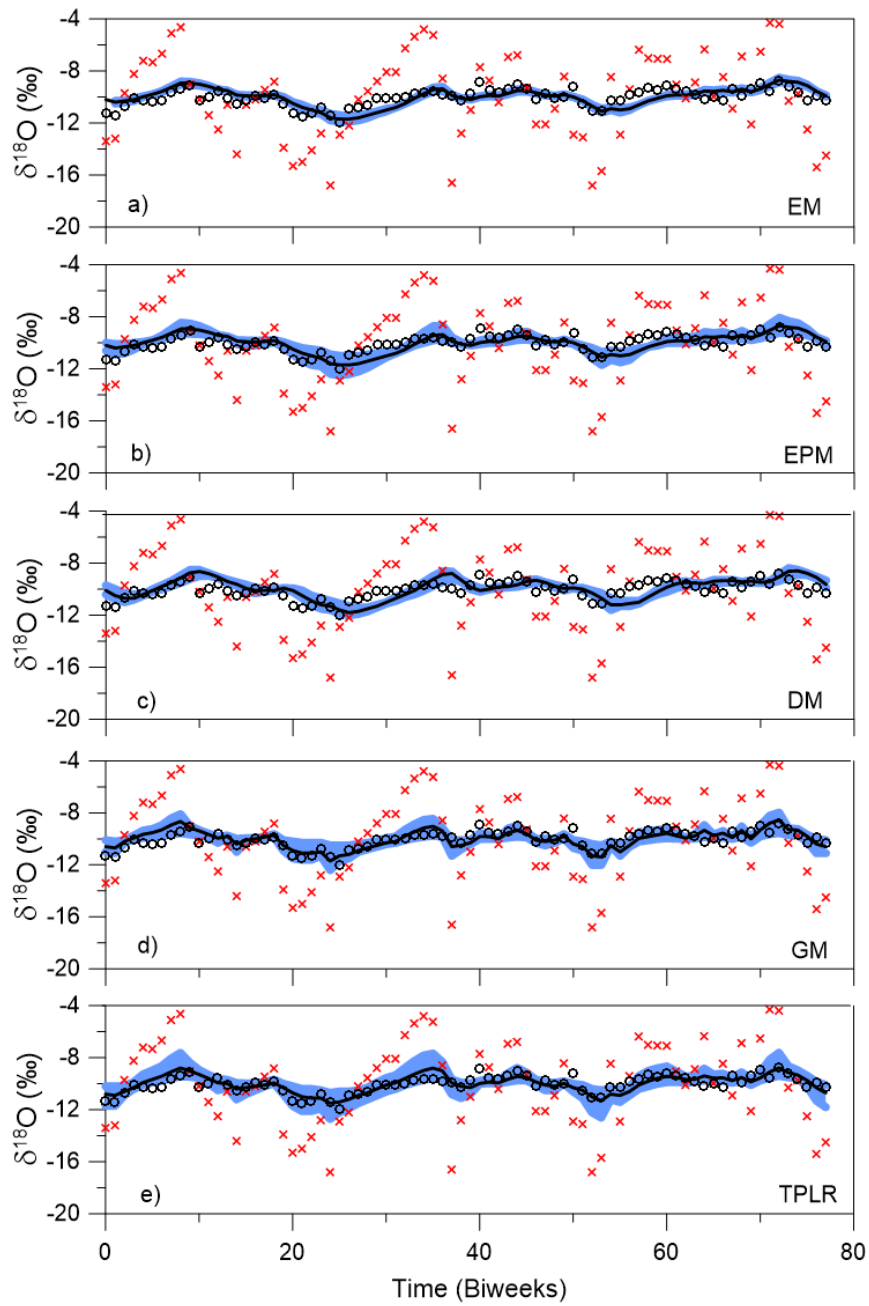
Figure 3. Fitted results of the five lumped parameter models used to simulate the temporal variability in the $\delta^{18}O$ streamflow composition at the outlet of the basin (M8). (a) Exponential model (EM); (b) exponential-piston model (EPM); (c) dispersion model (DM); (d) gamma model (GM); and (e) two parallel linear reservoir model (TPLR). The open circles represent the observed isotopic composition in streamflow; the red crosses represent the isotopic composition in precipitation; the black line represents the best simulated isotopic composition

1　in streamflow according to the KGE (Gupta et al., 2009) objective function; and the blue

2　shaded area corresponds to the 5-95% confidence limits of the possible solutions from the

3　parameter sets within the range of behavioral solutions, i.e., solutions which yield at least
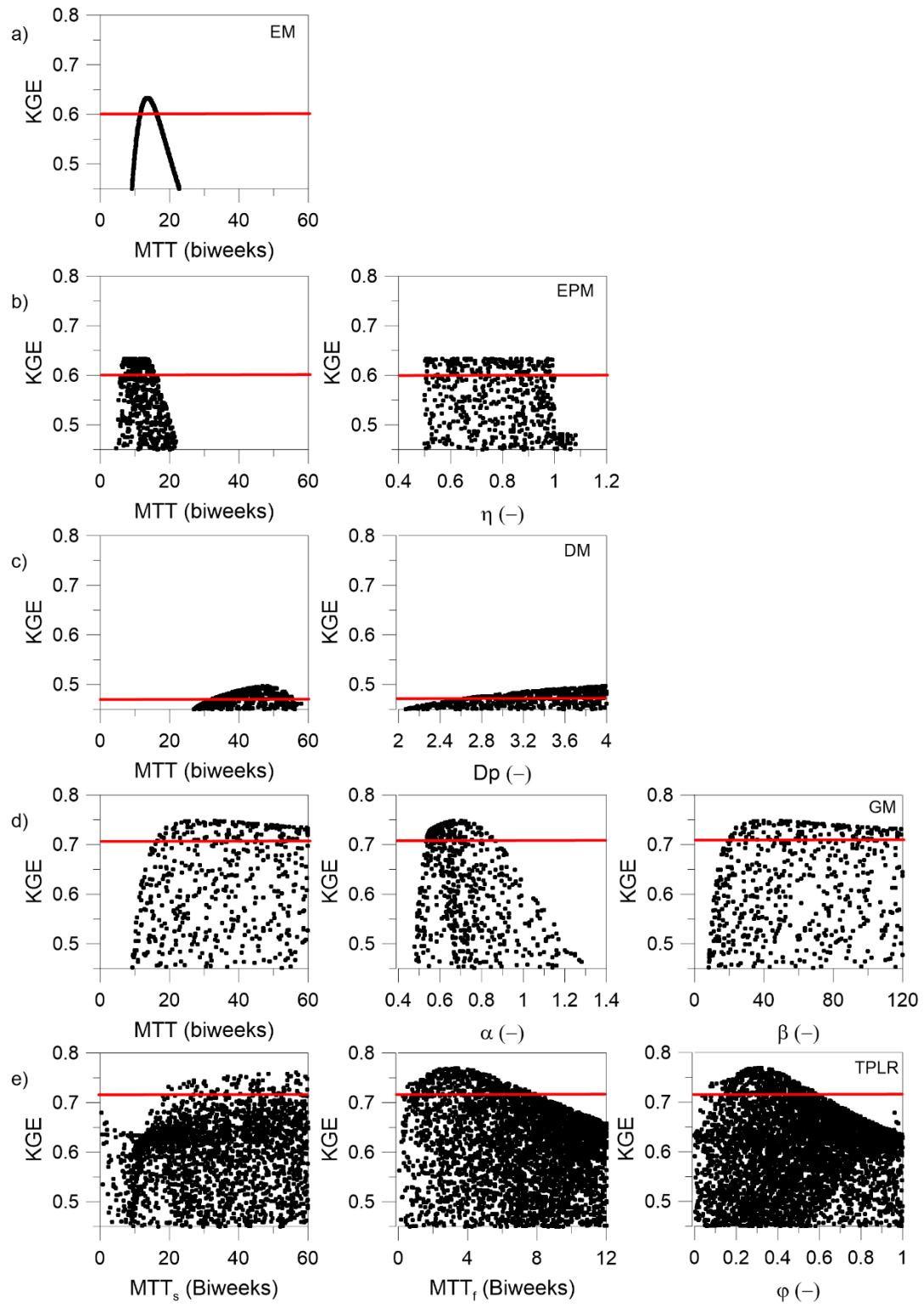
4　95% KGE.

Figure 4. Monte Carlo simulations of the fitted parameters of the five lumped parameter models used to simulate the δ^{18}O streamflow composition at the outlet of the basin (M8). a)

1 EM; b) EPM; c) DM; d) GM; and e) TPLR. The (-) symbol in the x-axes denotes that fitting

2 parameter is dimensionless. Horizontal red lines indicate threshold of behavioral solutions (at
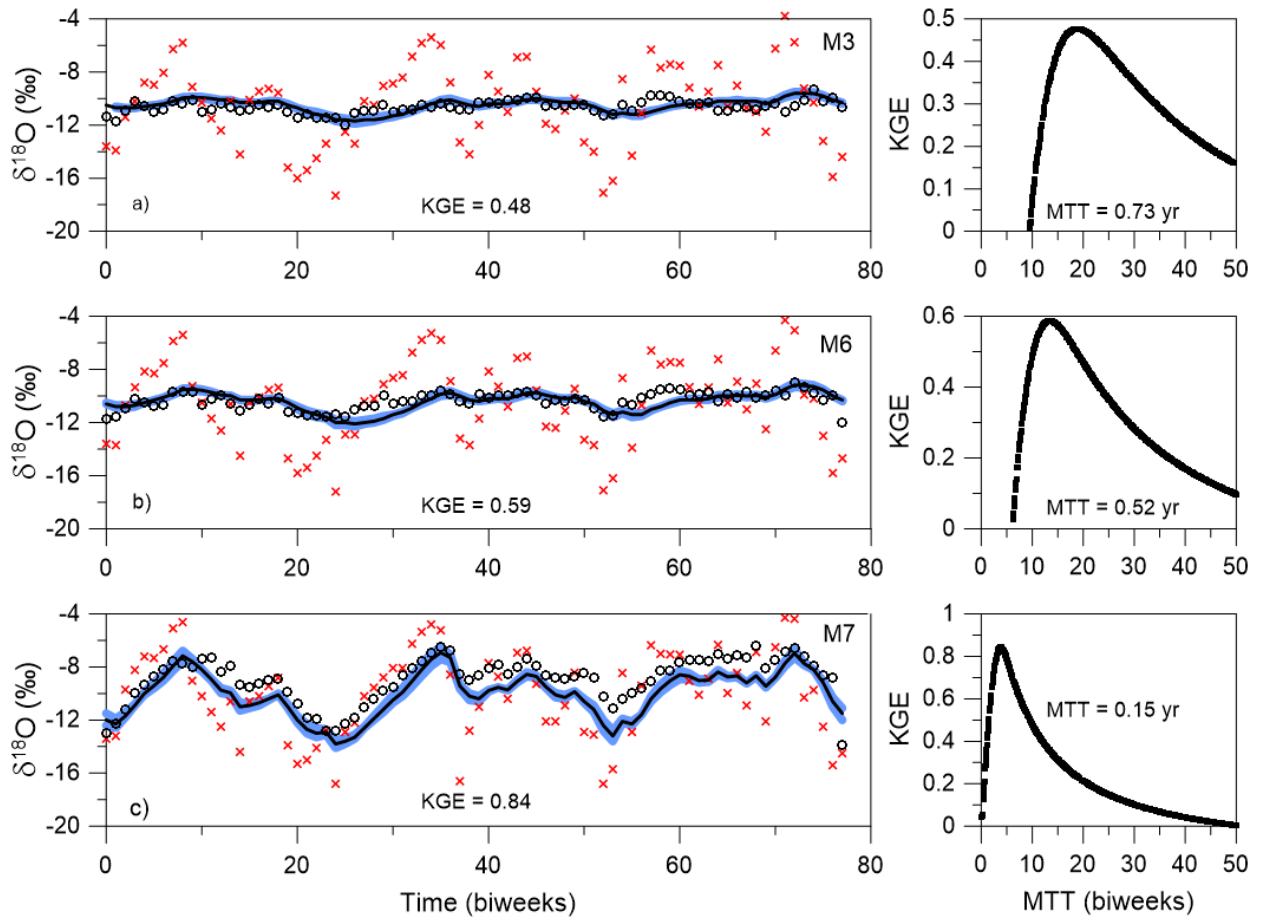
3 least 0.95 of maximum KGE).

1

Figure 5. Fitted results and Monte Carlo simulations of the fitted parameters of the
exponential model (EM) used to simulate the $\delta^{18}O$ streamflow composition in the catchments:
a) M3; b) M6; and c) M7. The open circles represent the observed isotopic composition in
streamflow; the red crosses represent the isotopic composition in precipitation; the black line
represents the best simulated isotopic composition in streamflow according to the KGE
objective function; and the blue shaded area corresponds to the 5-95% confidence limits of
the possible solutions from the MTT fitting parameters within the range of behavioral
solutions, i.e., solutions which yield at least 95% KGE. Panels on the right represent the
explored parameter range for the MTT parameter and the KGEs associated to each of them.

11
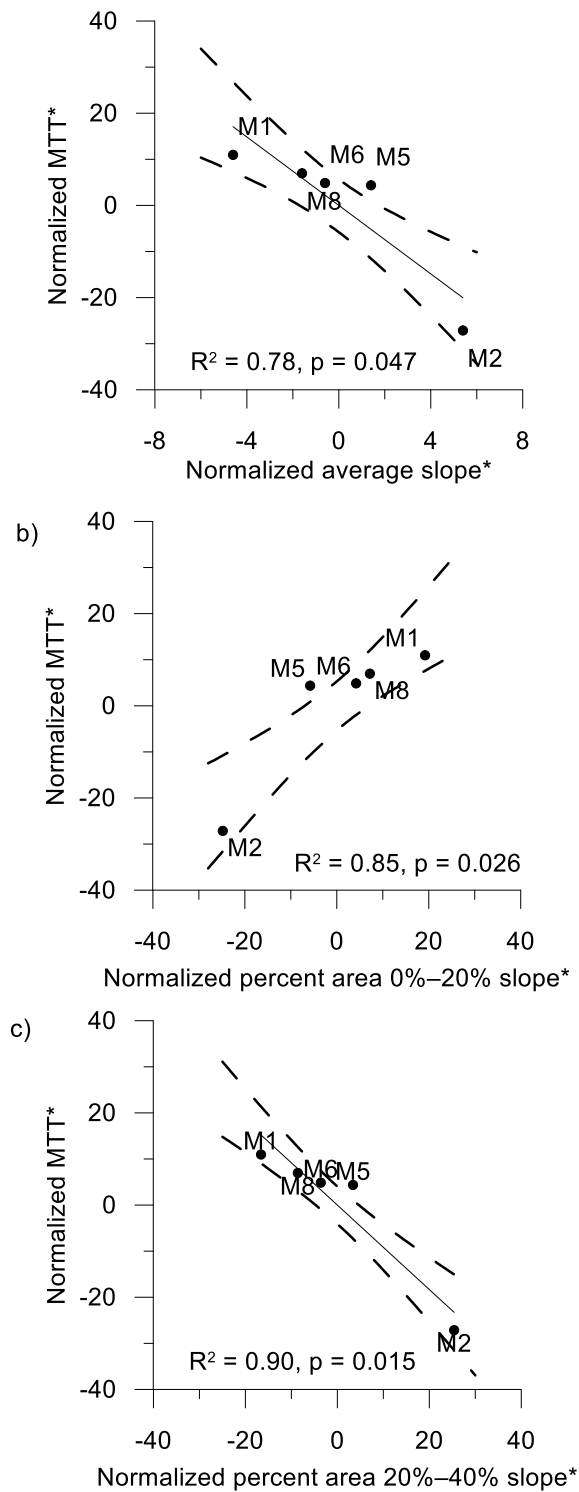
Figure 6. Correlations between mean transit time (MTT) and topographic indexes of the catchments: a) average catchment slope; b) catchment area with slopes between 0% and 20%;

1 and c) catchment area with slopes between 20% and 40%. Catchments M3 and M4 (additional

2 spring water source, see Figure 1) and M7 (at a flat hilltop disconnected from the hillslopes)

3 are not included in the regressions. Solid lines are linear regressions and dashed lines are the

4 90% confidence intervals of the regressions. * Indicates parameters are normalized by their

5 mean.

6
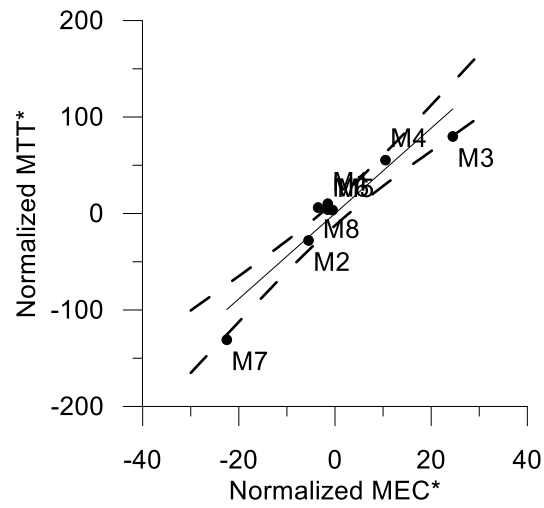
Figure 7. Correlation between mean transit time (MTT) and mean electrical conductivity (MEC) for weekly measurements of stream water samples collected during three years (June 2012-June 2015). Solid line is the linear regression and the dashed lines are the 90% confidence intervals of the regression. * Indicates parameters are normalized by their mean.